Spatial densities of momentum and forces in spin-one hadrons

Adam Freese[1,*] and Wim Cosyn[2,3,†]

[1]*Department of Physics, University of Washington, Seattle, Washington 98195, USA*
[2]*Department of Physics, Florida International University, Miami, Florida 33199, USA*
[3]*Department of Physics and Astronomy, Ghent University, B9000 Gent, Belgium*

(Received 22 August 2022; accepted 16 November 2022; published 16 December 2022)

Densities associated with the energy-momentum tensor are calculated for spin-one targets. These calculations are done in a light front formalism, which accounts for relativistic effects due to boosts and allows for arbitrary spatial localization of the target. These densities include the distribution of momentum, angular momentum, and pressures over a two-dimensional plane transverse to the light front. Results are obtained for both longitudinally and transversely polarized targets, and the formalism is tailored to allow the possibility of massless targets. The momentum density and pressure distributions are calculated for a deuteron target in a light cone convolution model, with which the properties of this model (such as helicity dependence of the densities) is illustrated.

DOI: 10.1103/PhysRevD.106.114013

I. INTRODUCTION

The energy-momentum tensor (EMT) has become a major topic of interest in hadron physics. It touches on several major outstanding problems in the field, including the proton mass puzzle [1–7] and the proton spin puzzle [8–10]. It is also believed by some to contain information about the mechanical properties of hadrons, including the spatial distributions of pressures and shear stresses [11–13], as well as information about the mechanical stability of hadrons.

Most research into the EMT of hadrons has focused on the gravitational form factors (GFFs) of spin-zero and spin-half targets. This is understandable, since the proton is spin-half, and spin-zero is an especially simple case for exploratory studies. However, spin-one targets play an important role in our understanding of the strong nuclear force, and are thus deserving of more attention in research on GFFs. The deuteron is spin-one after all, and as the simplest nucleus, it is an ideal testing ground for studies of how the internucleon force arises from quantum chromodynamics [14]. Spin-one targets more generally contain extra information not present in lower-spin targets, such as a gluon transversity distribution whose evolution decouples from quarks [15].

Several recent theoretical studies [16–19] and model calculations [20–23] have been done for the EMT and GFFs of spin-one targets. However, there is yet no investigation into the light front densities associated with the GFFs of spin-one targets. Breit frame studies exist [17,18], but there is considerable controversy regarding the physical meaningfulness of Breit frame densities (see Refs. [24–31] for a variety of perspectives), whereas light front densities have a clear physical meaning and interpretation as true densities [25,26,30,32,33]. It is thus prudent to investigate the light front densities associated with the GFFs of spin-one targets.

This work is an investigation into the general properties and expressions for EMT densities in spin-one targets. A companion paper [34] investigates the densities for a photon target specifically.

This paper is organized into the following sections. Section II considers the decomposition of EMT matrix elements into GFFs, examining how this decomposition depends on target polarization. Section III then obtains all the relevant densities, including static moments and radii, as well as their polarization dependence. Section IV illustrates some of these densities with a simple light cone convolution model of the deuteron, and Sec. V concludes the work.

II. MATRIX ELEMENTS FOR DEFINITE-SPIN STATES

For a massive spin-one system, the matrix element of the conserved, symmetric EMT between spin-one plane wave states is given by [16–18,20,21,35]

*afreese@uw.edu
†wcosyn@fiu.edu

Published by the American Physical Society under the terms of the Creative Commons Attribution 4.0 International license. Further distribution of this work must maintain attribution to the author(s) and the published article's title, journal citation, and DOI. Funded by SCOAP³.

$$\langle p'\lambda'|T^{\mu\nu}(0)|p\lambda\rangle = 2P^\mu P^\nu\left[-(\varepsilon\cdot\varepsilon'^*)\mathcal{G}_1(t) + \frac{(\varepsilon\cdot\Delta)(\varepsilon'^*\cdot\Delta)}{2M^2}\mathcal{G}_2(t)\right] + \frac{\Delta^\mu\Delta^\nu - \Delta^2 g^{\mu\nu}}{2}\left[-(\varepsilon\cdot\varepsilon'^*)\mathcal{G}_3(t) + \frac{(\varepsilon\cdot\Delta)(\varepsilon'^*\cdot\Delta)}{2M^2}\mathcal{G}_4(t)\right] + \frac{1}{2}P^{\{\mu}[\varepsilon'^{*\nu\}}(\varepsilon\cdot\Delta) - \varepsilon^{\nu\}}(\varepsilon'^*\cdot\Delta)]\mathcal{G}_5(t) + \frac{1}{4}[\Delta^{\{\mu}(\varepsilon'^{*\nu\}}(\varepsilon\cdot\Delta) + \varepsilon^{\nu\}}(\varepsilon'^*\cdot\Delta)) - \varepsilon^{\{\mu}\varepsilon'^{*\nu\}}\Delta^2 - 2g^{\mu\nu}(\varepsilon\cdot\Delta)(\varepsilon'^*\cdot\Delta)]\mathcal{G}_6(t), \tag{1}$$

where $P = \frac{1}{2}(p + p')$, $\Delta = p' - p$, $t = \Delta^2$, where ε is a polarization four-vector that depends on momentum p and spin quantum number λ, and ε' similarly on p' and λ', and where $\{\}$ denotes symmetrization without a factor $\frac{1}{2}$ (i.e., $a^{\{\mu}b^{\nu\}} = a^\mu b^\nu + a^\nu b^\mu$). Note that several conventions exist in the literature for naming the gravitational form factors. We have here used the notation first found in Ref. [16] and later adopted (and expanded) in Refs. [17,21]. Reference [18] gives a comparison of the existing conventions. Several nonconserved form factors, namely $\mathcal{G}_{7-9}(t)$, also exist when examining the EMT contributions of a single parton flavor, but in this work we examine only the total EMT, which is conserved. The effects of nonconserved GFFs on partonic densities are deferred to a future study. Reference [17] additionally gives two more form factors, $\mathcal{G}_{10,11}(t)$ for the asymmetric EMT, but a consistent application of Noether's second theorem to obtain the EMT has been shown to reproduce the symmetric Belinfante EMT for QCD [36], so we limit our attention to the symmetric EMT here.

Clearly, Eq. (1) is not applicable to massless systems, due to the presence of factors $1/M^2$. The presence of these factors is somewhat artificial; standard form factor decompositions like Eq. (1) are designed so that (1) the form factors are unitless and (2) poles do not occur in the form factors nor in accompanying Lorentz structures that are not present in the EMT matrix element. Condition (2) precludes using factors of $1/t$ instead of $1/M^2$ to accompany, e.g., $\mathcal{G}_2(t)$. However, if condition (1) is relaxed, one can write a variant of Eq. (1) with no factors of $1/M^2$ present, but several unitful Lorentz scalar functions.

This work will examine light front densities of spin-one systems, including massless systems such as the photon. It is thus desirable to have a breakdown into Lorentz scalar functions that is applicable to both massless and massive systems. When considering light front densities in particular, where $\Delta^+ = 0$ by virtue of integrating out x^- [30], the EMT matrix element can be decomposed as follows:

$$\langle p'\lambda'|T^{\mu\nu}(0)|p\lambda\rangle|_{\Delta^+=0} = 2P^\mu P^\nu \mathcal{A}_{\lambda'\lambda}(\boldsymbol{\Delta}_\perp) - i\frac{P^{\{\mu}\epsilon^{\nu\}P\Delta n}}{(P\cdot n)}\mathcal{J}_{\lambda'\lambda}(\boldsymbol{\Delta}_\perp) + \frac{\Delta^\mu\Delta^\nu - \Delta^2 g^{\mu\nu}}{2}\mathcal{D}_{\lambda'\lambda}(\boldsymbol{\Delta}_\perp) + \frac{P^{\{\mu}n^{\nu\}}}{(P\cdot n)}\mathcal{E}_{\lambda'\lambda}(\boldsymbol{\Delta}_\perp) + \frac{n^\mu n^\nu}{(P\cdot n)^2}\mathcal{H}_{\lambda'\lambda}(\boldsymbol{\Delta}_\perp) + i\frac{n^{\{\mu}\epsilon^{\nu\}P\Delta n}}{(P\cdot n)^2}\mathcal{K}_{\lambda'\lambda}(\boldsymbol{\Delta}_\perp), \tag{2}$$

where n is the lightlike four-vector that defines the light front coordinates, i.e., such that $V\cdot n = V^+$ and the decomposition was constructed to be invariant under scaling n by a factor. It should be remarked that the Lorentz scalar functions $\mathcal{A}_{\lambda'\lambda}(\boldsymbol{\Delta}_\perp)$ etc. are not proper form factors, owing to their dependence on the initial and final target helicities, but can more accurately be called helicity amplitudes. It should also be noted that this decomposition is not defined when $P^+ = 0$, which can occur in the massless case for plane waves in the $-z$ direction. This decomposition has several unitful helicity amplitudes, namely $\mathcal{E}$, $\mathcal{H}$ and $\mathcal{K}$, with units GeV^2, GeV^4 and GeV^2, respectively.

It should be stressed that we do not propose the helicity amplitudes in Eq. (2) as a replacement for any of the existing conventions; their utility lies specifically in the ability to take light front Fourier transformations of these helicity amplitudes to obtain physically interpretable densities. In the respect that Fourier transforms of these quantities produce light front densities (similarly to form factors for spin-zero and spin-half targets), we will occasionally refer to the helicity amplitudes as "effective form factors", but we stress that these quantities are not really proper form factors.

In the massive case, the six helicity amplitudes in Eq. (2) are linear combinations of the form factors found in Eq. (1), with the particular combination depending on the initial and final helicity. Of special interest are those that contribute to the Galilean densities [27,30], which are the densities corresponding to only the $+$ and transverse spatial components of the EMT. These densities have the special property of being covariant under the Galilean subgroup of

the Poincaré group. Since $n^+ = 0$ and $\mathbf{n}_\perp^i = 0$ (we use bold vectors with a $_\perp$ subscript to signify transverse spatial components), only $\mathcal{A}$, $\mathcal{J}$, and $\mathcal{D}$ contribute to these densities.

The relationships between the form factors in Eq. (1) and helicity amplitudes in Eq. (2) can be found by evaluating Eq. (1) explicitly using the spin-one polarization vectors found in Ref. [37] at $\xi \equiv -\frac{\Delta^+}{2P^+} = 0$ (which are also given in Appendix A). For example, let us consider cases with no helicity flip ($\lambda' = \lambda$), which are relevant to the Galilean densities of light front helicity states. For helicity ± 1 states we have

$$\mathcal{A}_{\pm\pm}(\mathbf{\Delta}_\perp) = \mathcal{G}_1(t) - \frac{t}{4M^2}\mathcal{G}_2(t), \tag{3a}$$

$$\mathcal{J}_{\pm\pm}(\mathbf{\Delta}_\perp) = \pm\frac{1}{2}\mathcal{G}_5(t) \equiv \pm\mathcal{J}(t), \tag{3b}$$

$$\mathcal{D}_{\pm\pm}(\mathbf{\Delta}_\perp) = \mathcal{G}_3(t) - \mathcal{G}_6(t) - \frac{t}{4M^2}\mathcal{G}_4(t), \tag{3c}$$

whereas for helicity-0 states we have

$$\mathcal{A}_{00}(\mathbf{\Delta}_\perp) = \left(1 + \frac{t}{2M^2}\right)\mathcal{G}_1(t) - \frac{t}{4M^2}(2\mathcal{G}_5(t) + \mathcal{G}_6(t)) - \frac{t^2}{8M^4}\mathcal{G}_2(t), \tag{4a}$$

$$\mathcal{J}_{00}(\mathbf{\Delta}_\perp) = 0, \tag{4b}$$

$$\mathcal{D}_{00}(\mathbf{\Delta}_\perp) = \mathcal{G}_3(t) - \frac{t}{4M^2}(-2\mathcal{G}_3(t) + \mathcal{G}_6(t)) - \frac{t^2}{8M^4}\mathcal{G}_4(t). \tag{4c}$$

The results for the other helicity amplitudes can be found in Appendix B.

A. Transversely polarized states

We next consider transversely polarized states for *massive* spin-one hadrons. Since the only sensible quantization axis for the spin of massless particles is along the direction of travel, transversely polarized states can only sensibly be considered in the massive case. The transverse polarization vectors are given by the following linear combinations of light front helicity states [38],

$$\varepsilon^\mu_{T,\pm 1} = \frac{\varepsilon_{+1} \pm \sqrt{2}e^{i\phi_s}\varepsilon_0 + e^{2i\phi_s}\varepsilon_{-1}}{2}, \tag{5a}$$

$$\varepsilon^\mu_{T,0} = \frac{\varepsilon_{+1} - e^{2i\phi_s}\varepsilon_{-1}}{\sqrt{2}}, \tag{5b}$$

and similarly for the final (primed) state. Accordingly, the relevant EMT matrix elements will involve spin-flip contributions. A catalog of all the individual contributions can be found in Appendix B. Without loss of generality, we can define $\hat{x} = \mathbf{s}_\perp$, and for more compact formulas, we suppress explicit $\mathbf{s}_\perp$ dependence in the expressions to follow.

The simplest manner to give results is in terms of the effective form factors,

$$\langle p', m_s|T^{\mu\nu}(0)|p, m_s\rangle = 2P^\mu P^\nu \mathcal{A}_T^{(m_s)}(\mathbf{\Delta}_\perp) - i\frac{P^{\{\mu}\epsilon^{\nu\}P\Delta n}}{(P\cdot n)}\mathcal{J}_T^{(m_s)}(\mathbf{\Delta}_\perp) + \frac{\Delta^\mu\Delta^\nu - \Delta^2 g^{\mu\nu}}{2}\mathcal{D}_T^{(m_s)}(\mathbf{\Delta}_\perp) + \frac{P^{\{\mu}n^{\nu\}}}{(P\cdot n)}\mathcal{E}_T^{(m_s)}(\mathbf{\Delta}_\perp) + \frac{n^\mu n^\nu}{(P\cdot n)^2}\mathcal{H}_T^{(m_s)}(\mathbf{\Delta}_\perp) + i\frac{n^{\{\mu}\epsilon^{\nu\}P\Delta n}}{(P\cdot n)^2}\mathcal{K}_T^{(m_s)}(\mathbf{\Delta}_\perp), \tag{6}$$

where $m_s \in \{-1, 0, +1\}$ is the magnetic spin number, i.e., the eigenvalue of $\mathbf{s}_\perp$ projected along the quantization axis. Each of the effective form factors works out to have the form,

$$\mathcal{F}_T^{(\pm 1)}(\mathbf{\Delta}_\perp) = \frac{1}{4}(\mathcal{F}_{++}(t) + \mathcal{F}_{--}(t) + 2\mathcal{F}_{00}(t)) + \frac{t\cos 2\phi_\Delta}{8M^2}\mathcal{F}_T^{\cos 2\phi}(t) \pm \frac{i\sqrt{-t}\sin\phi_\Delta}{2M}\mathcal{F}_T^{\sin\phi}(t), \tag{7a}$$

$$\mathcal{F}_T^{(0)}(\mathbf{\Delta}_\perp) = \frac{1}{2}(\mathcal{F}_{++}(t) + \mathcal{F}_{--}(t)) - \frac{t\cos 2\phi_\Delta}{4M^2}\mathcal{F}_T^{\cos 2\phi}(t), \tag{7b}$$

where $\mathcal{F}$ stands in for any of the effective form factors in Eq. (2) or Eq. (6), and where ϕ_Δ is the angle between $\mathbf{\Delta}_\perp$ and $\mathbf{s}_\perp$. The $\mathcal{F}_T^{\sin\phi}(t)$ and $\mathcal{F}_T^{\cos 2\phi}(t)$ that are relevant to the Galilean light front densities are, in terms of the traditional GFFs,

$$\mathcal{A}_T^{\sin\phi}(t) = \mathcal{G}_5(t) - 2\mathcal{G}_1(t) + \frac{t}{2M^2}\mathcal{G}_2(t), \tag{8a}$$

$$\mathcal{A}_T^{\cos 2\phi}(t) = \mathcal{G}_2(t), \tag{8b}$$

$$\mathcal{J}_T^{\sin\phi}(t) = 0, \tag{8c}$$

$$\mathcal{J}_T^{\cos 2\phi}(t) = 0, \tag{8d}$$

$$\mathcal{D}_T^{\sin\phi}(t) = \mathcal{G}_6(t) - 2\mathcal{G}_3(t) + \frac{t}{2M^2}\mathcal{G}_4(t), \tag{8e}$$

$$\mathcal{D}_T^{\cos 2\phi}(t) = \mathcal{G}_4(t). \tag{8f}$$

It should be clear from these results, combined with Eqs. (3b) and (4b), that $\mathcal{J}_T = 0$. This means that the J_z density for transversely polarized states is zero, see Eq. (16b) further down. To be sure, the structure of Eq. (2) means that $\mathcal{J}_T$ is a J_z density of transversely polarized states and not a density of transverse angular momentum. This finding is not surprising, since the expectation value of J_z in a transversely polarized state is zero. The transverse angular momentum operator is given by $x^- T^{+i}(x) - x_\perp^i T^{+-}(x)$, meaning that this would entail a non-Galilean density and is thus beyond the scope of this work. Indeed, this quantity would involve several of the non-Galilean helicity amplitudes (those other than $\mathcal{A}$, $\mathcal{J}$ and $\mathcal{D}$).

It may be instructive to consider Eq. (7) in terms of unpolarized, vector polarized, and tensor polarized combinations of the target. These polarization combinations are defined for transversely polarized targets as follows:

$$\mathcal{F}_T^{(U)}(\mathbf{\Delta}_\perp) = \frac{1}{3}(\mathcal{F}_T^{(+1)}(\mathbf{\Delta}_\perp) + \mathcal{F}_T^{(-1)}(\mathbf{\Delta}_\perp) + \mathcal{F}_T^{(0)}(\mathbf{\Delta}_\perp)), \tag{9a}$$

$$\mathcal{F}_T^{(V)}(\mathbf{\Delta}_\perp) = \mathcal{F}_T^{(+1)}(\mathbf{\Delta}_\perp) - \mathcal{F}_T^{(-1)}(\mathbf{\Delta}_\perp), \tag{9b}$$

$$\mathcal{F}_T^{(T)}(\mathbf{\Delta}_\perp) = \frac{1}{2}(2\mathcal{F}_T^{(0)}(\mathbf{\Delta}_\perp) - \mathcal{F}_T^{(+1)}(\mathbf{\Delta}_\perp) - \mathcal{F}_T^{(-1)}(\mathbf{\Delta}_\perp)). \tag{9c}$$

If we also define these states for longitudinally polarized targets,

$$\mathcal{F}_L^{(U)}(t) = \frac{1}{3}(\mathcal{F}_{++}(t) + \mathcal{F}_{--}(t) + \mathcal{F}_{00}(t)), \tag{10a}$$

$$\mathcal{F}_L^{(V)}(t) = \mathcal{F}_{++}(t) - \mathcal{F}_{--}(t), \tag{10b}$$

$$\mathcal{F}_L^{(T)}(t) = \frac{1}{2}(2\mathcal{F}_{00}(t) - \mathcal{F}_{++}(t) - \mathcal{F}_{--}(t)), \tag{10c}$$

then we find for the transversely polarized states that

$$\mathcal{F}_T^{(U)}(\mathbf{\Delta}_\perp) = \mathcal{F}_L^{(U)}(t) \tag{11a}$$

$$\mathcal{F}_T^{(V)}(\mathbf{\Delta}_\perp) = \frac{i\sqrt{-t}\sin\phi_\Delta}{M}\mathcal{F}_T^{\sin\phi}(t) \tag{11b}$$

$$\mathcal{F}_T^{(T)}(\mathbf{\Delta}_\perp) = -\mathcal{F}_L^{(T)}(t) - \frac{t\cos 2\phi_\Delta}{4M^2}\mathcal{F}_T^{\cos 2\phi}(t). \tag{11c}$$

The modulations can thus be interpreted in terms of vector and tensor polarization states, but these states actually differ depending on the spin quantization axis. We will consider general polarization below. Throughout the remainder of this work, however, we focus on deuterons in specific polarization states rather than mixtures. The reason for this is that unpolarized, vector polarized, and tensor polarized states are mixtures that are not present in the Hilbert space of the target, and we choose to focus in this work on the densities and properties of spin-one systems in pure states.

B. General polarization

An alternate way of considering the dependence on the initial and final state helicities of the spin-one particle in Eq. (2) is by tracing it with a spin-one density matrix $\rho(\lambda, \lambda')$ characterizing the ensemble,

$$\langle\langle T^{\mu\nu}(0)\rangle\rangle \equiv \sum_{\lambda,\lambda'}\rho(\lambda,\lambda')\langle p'\lambda'|T^{\mu\nu}(0)|p\lambda\rangle. \tag{12}$$

We refer the reader to Appendix C for a summary of the spin-one density matrix formalism and a definition of the density matrix parameters ($S_L, S_T, \phi_S, T_{LL}, T_{LT}, T_{TT}, \phi_{T_L}, \phi_{T_T}$) appearing in the formulas that follow. By considering the relevant contractions of the off-diagonal covariant density matrix of Eq. (C12), evaluated at $\Delta^+ = 0$, with tensors built from P, Δ, n and the 4D Levi-Civita tensor, we obtain the following expressions for the density matrix averaged effective form factors appearing in Eq. (2),

$$\begin{aligned}\sum_{\lambda,\lambda'}\rho(\lambda,\lambda')\mathcal{A}_{\lambda'\lambda} = {} & \left(\frac{2}{3} + T_{LL}\right)\left(\mathcal{G}_1(t) - \frac{t}{4M^2}\mathcal{G}_2(t)\right) + \left(\frac{1}{3} - T_{LL}\right)\left[\left(1 + \frac{t}{2M^2}\right)\mathcal{G}_1(t) - \frac{t^2}{8M^4}\mathcal{G}_2(t)\right. \\ & \left. - \frac{t}{2M^2}\mathcal{G}_5(t) - \frac{t}{4M^2}\mathcal{G}_6(t)\right] + iS_T\sin(\phi_S - \phi_t)\frac{\sqrt{-t}}{M}\left(\mathcal{G}_1(t) - \frac{t}{4M^2}\mathcal{G}_2(t) - \frac{\mathcal{G}_5(t)}{2}\right) \\ & + T_{TT}\cos(2\phi_{T_T} - 2\phi_t)\frac{t}{4M^2}\mathcal{G}_2(t),\end{aligned} \tag{13a}$$

$$\sum_{\lambda,\lambda'}\rho(\lambda,\lambda')\mathcal{J}_{\lambda'\lambda} = \frac{S_L}{2}\mathcal{G}_5(t) + iT_{LT}\sin(\phi_{T_L}-\phi_t)\frac{\sqrt{-t}}{2M}(\mathcal{G}_5(t)+\mathcal{G}_6(t)), \tag{13b}$$

$$\begin{aligned}\sum_{\lambda,\lambda'}\rho(\lambda,\lambda')\mathcal{D}_{\lambda'\lambda} = {}& \left(\frac{2}{3}+T_{LL}\right)\left(\mathcal{G}_3(t)-\frac{t}{4M^2}\mathcal{G}_4(t)-\mathcal{G}_6(t)\right)+\left(\frac{1}{3}-T_{LL}\right)\left[\left(1+\frac{t}{2M^2}\right)\mathcal{G}_3(t)\right.\\ &\left.-\frac{t^2}{8M^4}\mathcal{G}_4(t)-\frac{t}{4M^2}\mathcal{G}_6(t)\right]+iS_T\sin(\phi_S-\phi_t)\frac{\sqrt{-t}}{M}\left(\mathcal{G}_3(t)-\frac{t}{4M^2}\mathcal{G}_4(t)-\frac{\mathcal{G}_6(t)}{2}\right)\\ &+T_{TT}\cos(2\phi_{T_T}-2\phi_t)\frac{t}{4M^2}\mathcal{G}_4(t),\end{aligned} \tag{13c}$$

where ϕ_t is the azimuthal angle of $\mathbf{\Delta}_\perp$.

We point out that $\mathcal{A}$ and $\mathcal{D}$ depend on the same density matrix parameters—namely, 1 (the unpolarized part), $T_{LL}, S_T\sin(\phi_S-\phi_t)$, and $T_{TT}\cos(2\phi_{T_T}-2\phi_t)$—while $\mathcal{J}$ depends on S_L and $T_{LT}\sin(\phi_{T_L}-\phi_t)$. The first set of parameters are scalars and the second set are pseudoscalars, reflecting the parity properties of the central charge p^+ and pressure on the one hand, and particle spin on the other. The modulations in the densities for the transversely polarized states are identified with the transverse vector ($S_T\sin\phi$) and mixed longitudinal-transverse tensor ($T_{LT}\sin\phi$) polarized part of the density matrix for the $\sin\phi$ modulations, and the completely transverse tensor part ($T_{TT}\cos 2\phi$) for the $\cos 2\phi$ modulations.

For Eq. (13), our previous expressions for the helicity [Eqs. (3) and (4)] and transversely polarized states [Eqs. (7) and (8)] are recovered after identifying the corresponding density matrix parameters for these ensembles. For pure longitudinal polarized states we need the following rest frame spin parameters

$$\lambda=\pm1:\qquad S_L=\pm1, T_{LL}=1/3,\quad S_T=T_{LT}=T_{TT}=0, \tag{14a}$$

$$\lambda=0:\qquad T_{LL}=-2/3,\quad S_L=S_T=T_{LT}=T_{TT}=0. \tag{14b}$$

For pure transversely polarized states one has

$$\lambda=\pm1:\qquad S_T=\pm1, T_{LL}=-1/6, T_{TT}=1/2,\quad \phi_{T_T}=\phi_S, S_L=T_{LT}=0, \tag{15a}$$

$$\lambda=0:\qquad T_{LL}=1/3, T_{TT}=-1, \phi_{T_T}=\phi_S,\quad S_T=S_L=T_{LT}=0. \tag{15b}$$

III. PROPERTIES OF SPIN-ONE DENSITIES

For states with definite light front helicity, the effective form factors as given in Eqs. (3) and (4) can be used to obtain the azimuthally symmetric light front P^+, angular momentum, and pressure densities of a spin-one system localized in the transverse plane. The formulas for the P^+ density and comoving stress tensor are identical to those already found in Refs. [27,30] for spin-zero or spin-half hadrons, but with $\mathcal{A}$ and $\mathcal{D}$ substituted for A and D. We give these relations again here (along with the angular momentum density)

$$\rho^{(\lambda)}_{p^+}(b_\perp) = P^+\int\frac{\mathrm{d}^2\mathbf{\Delta}_\perp}{(2\pi)^2}\mathcal{A}_{\lambda\lambda}(t)e^{-i\mathbf{\Delta}_\perp\cdot\mathbf{b}_\perp}, \tag{16a}$$

$$\rho^{(\lambda)}_{J_z}(b_\perp) = \lambda\int\frac{\mathrm{d}^2\mathbf{\Delta}_\perp}{(2\pi)^2}\left\{\mathcal{J}(t)+t\frac{\mathrm{d}\mathcal{J}(t)}{\mathrm{d}t}\right\}e^{-i\mathbf{\Delta}_\perp\cdot\mathbf{b}_\perp}, \tag{16b}$$

$$S^{ij}_\lambda(\mathbf{b}_\perp) = \frac{1}{4P^+}\int\frac{\mathrm{d}^2\mathbf{\Delta}_\perp}{(2\pi)^2}(\mathbf{\Delta}^i_\perp\mathbf{\Delta}^j_\perp-\mathbf{\Delta}^2_\perp\delta_{ij})\mathcal{D}_{\lambda\lambda}(t)e^{-i\mathbf{\Delta}_\perp\cdot\mathbf{b}_\perp}. \tag{16c}$$

The only significant difference from the spin-zero and spin-half cases is that the densities now depend on λ, meaning that the distribution of momentum, angular momentum, and forces will differ between spin-one hadrons of the same species that are prepared in different helicity states.

For transversely polarized states of massive hadrons, the effective form factors have azimuthal dependence. The exact manner of this dependence varies between the densities under consideration, so we will proceed to consider the properties of each separately.

A. Light front momentum density

The P^+ density for helicity states is given already by Eq. (16a). The transversely polarized P^+ density contains azimuthal dependence which is essentially carried over from the azimuthal dependence of the effective form factors, since

$$\int\frac{\mathrm{d}^2\mathbf{\Delta}_\perp}{(2\pi)^2}\frac{i\sqrt{-t}\sin\phi_\Delta}{2M}\mathcal{A}^{\sin\phi}_T(t)e^{-i\mathbf{\Delta}_\perp\cdot\mathbf{b}_\perp} = -\frac{\sin\phi}{2M}\frac{\mathrm{d}}{\mathrm{d}b_\perp}\int\frac{\mathrm{d}^2\mathbf{\Delta}_\perp}{(2\pi)^2}\mathcal{A}^{\sin\phi}_T(t)e^{-i\mathbf{\Delta}_\perp\cdot\mathbf{b}_\perp}, \tag{17a}$$

$$\int \frac{d^2\mathbf{\Delta}_\perp}{(2\pi)^2}\frac{t\cos 2\phi_\Delta}{4M^2}\mathcal{A}_T^{\cos 2\phi}(t)e^{-i\mathbf{\Delta}_\perp\cdot\mathbf{b}_\perp} = \frac{\cos 2\phi}{4M^2}\left\{\frac{d^2}{db_\perp^2}-\frac{1}{b_\perp}\frac{d}{db_\perp}\right\}\int\frac{d^2\mathbf{\Delta}_\perp}{(2\pi)^2}\mathcal{A}_T^{\cos 2\phi}(t)e^{-i\mathbf{\Delta}_\perp\cdot\mathbf{b}_\perp}, \tag{17b}$$

where on the right-hand side, ϕ is the angle between $\mathbf{b}_\perp$ and $\mathbf{s}_\perp$. In numerical applications, formulas involving derivatives may not be stable, and it may be more helpful to use Hankel transforms instead,

$$\int \frac{d^2\mathbf{\Delta}_\perp}{(2\pi)^2}\frac{i\sqrt{-t}\sin\phi_\Delta}{2M}\mathcal{A}_T^{\sin\phi}(t)e^{-i\mathbf{\Delta}_\perp\cdot\mathbf{b}_\perp} = \frac{\sin\phi}{2M}\frac{1}{2\pi}\mathcal{H}_1[k\mathcal{A}_T^{\sin\phi}(t=-k^2)](b_\perp), \tag{18a}$$

$$\int \frac{d^2\mathbf{\Delta}_\perp}{(2\pi)^2}\frac{t\cos 2\phi_\Delta}{4M^2}\mathcal{A}_T^{\cos 2\phi}(t)e^{-i\mathbf{\Delta}_\perp\cdot\mathbf{b}_\perp} = \frac{\cos 2\phi}{4M^2}\frac{1}{2\pi}\mathcal{H}_2[k^2\mathcal{A}_T^{\cos 2\phi}(t=-k^2)](b_\perp), \tag{18b}$$

where the Hankel transform of order ν is defined by [39]:

$$\mathcal{H}_\nu[F(k)](b) = \int_0^\infty dk k J_\nu(bk)F(k), \tag{19}$$

and where $J_\nu(x)$ is the Bessel function of order ν.

For the sake of more compact formulas, it is prudent to define

$$\rho_T^{\sin\phi}(b_\perp) = \frac{P^+}{2\pi}\frac{1}{2M}\mathcal{H}_1[k\mathcal{A}_T^{\sin\phi}(-k^2)](b_\perp), \tag{20a}$$

$$\rho_T^{\cos 2\phi}(b_\perp) = \frac{P^+}{2\pi}\frac{1}{4M^2}\mathcal{H}_2[k^2\mathcal{A}_T^{\cos 2\phi}(-k^2)](b_\perp). \tag{20b}$$

The P^+ density of a transversely polarized spin-one hadron is thus given by

$$\rho_T^{(\pm 1)}(\mathbf{b}_\perp) = \frac{\rho_{p^+}^{(+)}(b_\perp)+\rho_{p^+}^{(0)}(b_\perp)}{2} \pm \sin\phi\rho_T^{\sin\phi}(b_\perp) + \frac{1}{2}\cos 2\phi\rho_T^{\cos 2\phi}(b_\perp), \tag{21a}$$

$$\rho_T^{(0)}(\mathbf{b}_\perp) = \rho_{p^+}^{(+)}(b_\perp) - \cos 2\phi\rho_T^{\cos 2\phi}(b_\perp), \tag{21b}$$

where we have used $\rho_{p^+}^{(+)}(b_\perp) = \rho_{p^+}^{(-)}(b_\perp)$ to make the formulas slightly shorter.

The P^+ densities for all polarization states satisfy sum rules. Integrating Eq. (16a) over all space gives

$$\int d^2\mathbf{b}_\perp\rho_{p^+}^{(\lambda)}(b_\perp) = P^+\mathcal{A}_{\lambda\lambda}(0). \tag{22}$$

For this to equal P^+, we have the sum rule

$$\mathcal{A}_{\lambda\lambda}(0) = 1, \tag{23}$$

for each helicity λ. Since $\mathcal{A}(0) = \mathcal{G}_1(0)$ for massive hadrons, this is compatible with the $\mathcal{G}_1(0) = 1$ sum rule of Ref. [17]. Since the integrals of $\sin\phi$ and $\cos 2\phi$ over $[0, 2\pi)$ are zero, the azimuthal dependence of $\rho_T^{(m_s)}(\mathbf{b}_\perp, \mathbf{s}_\perp)$ integrates to zero, and we also have

$$\int d^2\mathbf{b}_\perp\rho_T^{(m_s)}(\mathbf{b}_\perp, \mathbf{s}_\perp) = P^+. \tag{24}$$

The P^+ density for both helicity and transversely polarized states do not have P^+ dipole moments, i.e., their center-of-P^+ is at the origin, as expected. A general explanation for why this occurs can be found in Sec. 7 of Ref. [40]. For the case of helicity states, it is easy to see that

$$\int d^2\mathbf{b}_\perp\mathbf{b}_\perp\rho_{p^+}^{(\lambda)}(b_\perp) = 0. \tag{25}$$

For transversely polarized states, if we use coordinates where $\mathbf{s}_\perp = \hat{x}$,

$$\int d^2\mathbf{b}_\perp\mathbf{b}_\perp\rho_T^{(m_s)}(\mathbf{b}_\perp, \mathbf{s}_\perp) = \frac{m_s\hat{y}P^+}{2M}(\mathcal{G}_5(0) - 2\mathcal{G}_1(0)) = 0. \tag{26}$$

We know $\mathcal{G}_1(0) = 1$ by momentum conservation. It has been shown previously [16,17,20] that $\mathcal{G}_5(0) = 2$ follows from angular momentum conservation. Thus, the center-of-P^+ is at the origin, as expected.

On the other hand, the transversely polarized P^+ density does exhibit a quadrupole moment. In two spatial dimensions, we define the traceless quadrupole tensor as

$$\mathcal{Q}_{\mathrm{LF}}^{ij}(\mathbf{s}_\perp, m_s) = \int d^2\mathbf{b}_\perp(2b_\perp^i b_\perp^j - b_\perp^2\delta_{ij})\rho_T^{(m_s)}(\mathbf{b}_\perp, \mathbf{s}_\perp). \tag{27}$$

The quadrupole moment itself can be identified with

$$\mathcal{Q}_{\mathrm{LF}}(\mathbf{s}_\perp, m_s) = s_\perp^i s_\perp^j\mathcal{Q}_{\mathrm{LF}}^{ij}(\mathbf{s}_\perp, m_s), \tag{28}$$

so that, conversely

$$\mathcal{Q}_{\mathrm{LF}}^{ij}(\mathbf{s}_\perp, m_s) = (2s_\perp^i s_\perp^j - \delta_{ij})\mathcal{Q}_{\mathrm{LF}}(\mathbf{s}_\perp, m_s). \tag{29}$$

We find through explicit evaluation that

$$\mathcal{Q}_{\rm LF}(\mathbf{s}_\perp, \pm 1) = \frac{P^+}{2M^2}\mathcal{G}_2(0) \equiv \frac{1}{2}\mathcal{Q}_{\rm LF}, \tag{30a}$$

$$\mathcal{Q}_{\rm LF}(\mathbf{s}_\perp, 0) = -\frac{P^+}{M^2}\mathcal{G}_2(0) \equiv -\mathcal{Q}_{\rm LF}. \tag{30b}$$

The value of $\mathcal{G}_2(0)$ is not constrained by any conservation laws or sum rules, and is zero for a free boson [18]. A nonzero quadrupole moment must thus be generated by dynamics.

As is conventional in the nuclear physics literature [41], a positive quadrupole moment indicates a prolate hadron (elongated in the direction of the spin quantization axis), while a negative quadrupole moment indicates an oblate hadron (flattened in the direction of the spin axis). A positive $\mathcal{G}_2(0)$ would thus mean that the $m_s = \pm 1$ state is prolate, and that the $m_s = 0$ state is oblate. A negative value for $\mathcal{G}_2(0)$ would of course indicate the opposite.

The contrast with the Breit frame mass quadrupole moment (see Refs. [17,18]) is remarkable. Comparing to Ref. [17] in particular[1] and using sum-rule enforced values (and dropping nonconserved form factors)

$$\mathcal{Q}_{\rm Breit} = \frac{1}{M}\left\{\mathcal{G}_2(0) - 1 - \frac{1}{2}\mathcal{G}_6(0)\right\}. \tag{31}$$

The Breit-frame quadrupole moment depends on $\mathcal{G}_6(0)$ in addition to $\mathcal{G}_2(0)$. Remarkably, $\mathcal{G}_6(0) = -2$ in the free theory [18], meaning that the Breit-frame mass quadrupole moment is also generated entirely by dynamics. However, since $\mathcal{G}_6(0)$ also comes into play, the quadrupole moment may turn out to have different magnitudes and even signs in the Breit frame and on the light front. In Ref. [21], the rho meson was found to have $\mathcal{G}_2^{\rm NJL}(0) \approx 0.158 > 0$ and $\mathcal{G}_6^{\rm NJL}(0) \approx -1$, which means that the rho meson (in this model) has a positive P^+ quadrupole moment on the light front, but a negative mass quadrupole moment in the Breit frame. Since $\mathcal{G}_6(0)$ is involved in the Breit-frame quadrupole moment, the difference between this and the light front quadrupole moment may be due to relativistic spin effects, as was remarked for the electric quadrupole moment in Ref. [42].

Let us lastly look at the P^+ radius of spin-one hadrons, which is defined through

$$\langle b_\perp^2\rangle_{P^+} = \frac{1}{P^+}\int {\rm d}^2\mathbf{b}_\perp \mathbf{b}_\perp^2 \rho_{p^+}(\mathbf{b}_\perp) = 4\frac{\partial \mathcal{A}(\mathbf{\Delta}_\perp)}{\partial t}\bigg|_{t=0}, \tag{32}$$

and for massive hadrons differs between polarization states, since the effective $\mathcal{A}(\mathbf{\Delta}_\perp)$ form factor differs. For helicity states of massive hadrons

$$\langle b_\perp^2\rangle_{P^+}(\lambda = \pm 1) = 4\frac{{\rm d}\mathcal{G}_1(t)}{{\rm d}t}\bigg|_{t=0} - \frac{\mathcal{G}_2(0)}{M^2}, \tag{33a}$$

$$\langle b_\perp^2\rangle_{P^+}(\lambda = 0) = 4\frac{{\rm d}\mathcal{G}_1(t)}{{\rm d}t}\bigg|_{t=0} + \frac{1}{M^2} \times (2\mathcal{G}_1(0) - 2\mathcal{G}_5(0) - \mathcal{G}_6(0)), \tag{33b}$$

while for transversely polarized states

$$\langle b_\perp^2\rangle_{P^+}(m_s = \pm 1) = \frac{1}{2}(\langle b_\perp^2\rangle_{P^+}(\lambda = \pm 1) + \langle b_\perp^2\rangle_{P^+}(\lambda = 0)), \tag{33c}$$

$$\langle b_\perp^2\rangle_{P^+}(m_s = 0) = \langle b_\perp^2\rangle_{P^+}(\lambda = \pm 1), \tag{33d}$$

The average P^+ density between the three polarization states (of massive hadrons) is the same for helicity and transversely polarized states,

$$\bar{\rho}_{p^+}(b_\perp) = \int \frac{{\rm d}^2\mathbf{\Delta}_\perp}{(2\pi)^2}\left\{\mathcal{G}_1(t) + \frac{t}{6M^2}\left(\mathcal{G}_1(t) - \mathcal{G}_2(t) - \mathcal{G}_5(t) - \frac{1}{2}\mathcal{G}_6(t)\right) - \frac{t^2}{24M^4}\mathcal{G}_2(t)\right\}e^{-i\mathbf{\Delta}_\perp\cdot\mathbf{b}_\perp}, \tag{34}$$

and likewise is the corresponding radius [21]

$$\overline{\langle b_\perp^2\rangle_{P^+}} = 4\frac{{\rm d}\mathcal{G}_1(t)}{{\rm d}t}\bigg|_{t=0} + \frac{2}{3M^2} \times \left(\mathcal{G}_1(0) - \mathcal{G}_2(0) - \mathcal{G}_5(0) - \frac{1}{2}\mathcal{G}_6(0)\right). \tag{35}$$

B. Angular-momentum density

The J_z angular-momentum density for helicity states is given in Eq. (16b), and for transversely polarized states is identically zero, as already discussed in Sec. II. As with the P^+ density, it may be helpful for numerical applications to be able to take a single Hankel transform of $\mathcal{J}(t)$ itself. Some straightforward algebra can be used to show that

$$\rho_{J_z}^{(\lambda)}(b_\perp) = \frac{\lambda b_\perp}{2\pi}\mathcal{H}_1[k\mathcal{J}(-k^2)](b_\perp). \tag{36}$$

From this density, the total angular momentum projected along the z axis is

$$\int {\rm d}^2\mathbf{b}_\perp \rho_{J_z}^{(\lambda)}(b_\perp) = \lambda\mathcal{J}(0) = \frac{\lambda}{2}\mathcal{G}_5(0). \tag{37}$$

Since this must be λ, we reproduce the finding of Refs. [16,17,20] that $\mathcal{G}_5(0) = 2$.

[1]The sign convention in Ref. [21] is the opposite as in Ref. [17], the latter of which we follow in this work.

For helicity $\lambda = \pm 1$ states, an angular momentum radius can be defined as

$$\langle b_\perp^2 \rangle_J = \frac{1}{\lambda}\int \mathrm{d}^2\mathbf{b}_\perp \mathbf{b}_\perp^2 \rho_{J_z}^{(\lambda)}(b_\perp) = 8\frac{\mathrm{d}\mathcal{J}(t)}{\mathrm{d}t}\bigg|_{t=0} = 4\frac{\mathrm{d}\mathcal{G}_5(t)}{\mathrm{d}t}\bigg|_{t=0}. \tag{38}$$

C. The comoving stress tensor

Following Refs. [13,30], the comoving stress tensor can most easily be dealt with using the following auxiliary density (which we call the Polyakov stress potential)

$$\tilde{\mathcal{D}}_\lambda(b_\perp) = \frac{1}{4P^+}\int \frac{\mathrm{d}^2\mathbf{\Delta}_\perp}{(2\pi)^2}\mathcal{D}_{\lambda\lambda}(t)e^{-i\mathbf{\Delta}_\perp\cdot\mathbf{b}_\perp}, \tag{39}$$

for which

$$S_\lambda^{ij}(\mathbf{b}_\perp) = (\mathbf{\nabla}_\perp^2\delta_{ij} - \mathbf{\nabla}_\perp^i\mathbf{\nabla}_\perp^j)\tilde{\mathcal{D}}_\lambda(b_\perp). \tag{40}$$

Analogously to spin-zero and spin-half helicity states [13,27,30], the comoving stress tensor for spin-one helicity states can be decomposed into an isotropic pressure $p(b_\perp)$ and shear stress (or pressure anisotropy) function $s(b_\perp)$ as follows:

$$S_\lambda^{ij}(\mathbf{b}_\perp) = \delta^{ij}p^{(\lambda)}(b_\perp) + \left(\frac{b_\perp^i b_\perp^j}{b_\perp^2} - \frac{1}{2}\delta^{ij}\right)s^{(\lambda)}(b_\perp). \tag{41}$$

This decomposition entails radial and tangential eigenpressures, given by

$$p_r^{(\lambda)}(b_\perp) = p^{(\lambda)}(b_\perp) + \frac{s^{(\lambda)}(b_\perp)}{2} = \frac{1}{b_\perp}\frac{\mathrm{d}\tilde{\mathcal{D}}_\lambda(b_\perp)}{\mathrm{d}b_\perp}, \tag{42a}$$

$$p_t^{(\lambda)}(b_\perp) = p^{(\lambda)}(b_\perp) - \frac{s^{(\lambda)}(b_\perp)}{2} = \frac{\mathrm{d}^2\tilde{\mathcal{D}}_\lambda(b_\perp)}{\mathrm{d}b_\perp^2}. \tag{42b}$$

As with the P^+ density, it may be helpful for numerical applications to obtain these quantities through higher-order Hankel transforms, rather than through derivatives. The isotropic pressure and shear stress can be shown to be

$$p^{(\lambda)}(b_\perp) = -\frac{1}{8P^+}\frac{1}{2\pi}\mathcal{H}_0[k^2\mathcal{D}_{\lambda\lambda}(-k^2)](b_\perp), \tag{43a}$$

$$s^{(\lambda)}(b_\perp) = -\frac{1}{4P^+}\frac{1}{2\pi}\mathcal{H}_2[k^2\mathcal{D}_{\lambda\lambda}(-k^2)](b_\perp). \tag{43b}$$

1. Transverse polarization

For transversely polarized states, the structure of the comoving stress tensor becomes significantly more complicated. The Polyakov stress potential obtains modulations completely analogous to those in the P^+ density; we define

$$\tilde{D}_T^{\sin\phi}(b_\perp) = \frac{1}{2\pi}\frac{1}{4P^+}\frac{1}{2M}\mathcal{H}_1[k\mathcal{D}_T^{\sin\phi}(-k^2)](b_\perp), \tag{44a}$$

$$\tilde{D}_T^{\cos 2\phi}(b_\perp) = \frac{1}{2\pi}\frac{1}{4P^+}\frac{1}{4M^2}\mathcal{H}_2[k^2\mathcal{D}_T^{\cos 2\phi}(-k^2)](b_\perp), \tag{44b}$$

where the effective form factor modulations are as defined in Eq. (8). The Polyakov potentials for transversely polarized states are given by

$$\tilde{D}_T^{(\pm 1)}(\mathbf{b}_\perp) = \frac{\tilde{D}_+(b_\perp) + \tilde{D}_0(b_\perp)}{2} \pm \sin\phi\tilde{D}_T^{\sin\phi}(b_\perp) + \frac{1}{2}\cos 2\phi\tilde{D}_T^{\cos 2\phi}(b_\perp), \tag{45a}$$

$$\tilde{D}_T^{(0)}(\mathbf{b}_\perp) = \tilde{D}_+(b_\perp) - \cos 2\phi\tilde{D}_T^{\cos 2\phi}(b_\perp), \tag{45b}$$

where we have used $\tilde{D}_+(b_\perp) = \tilde{D}_-(b_\perp)$ to make the formulas slightly shorter. The comoving stress tensor is then given by

$$S_T^{ij}(\mathbf{b}_\perp, m_s) = (\mathbf{\nabla}_\perp^2\delta_{ij} - \mathbf{\nabla}_\perp^i\mathbf{\nabla}_\perp^j)\tilde{\mathcal{D}}_T^{(m_s)}(\mathbf{b}_\perp). \tag{46}$$

This stress tensor no longer has the simple decomposition of Eq. (41); it contains a new tensor structure, and the functions multiplying each structure now contain azimuthal modulations,

$$S_T^{ij}(\mathbf{b}_\perp, m_s) = \delta^{ij}p_T^{(m_s)}(\mathbf{b}_\perp) + \left(\hat{b}^i\hat{b}^j - \frac{1}{2}\delta^{ij}\right)s_T^{(m_s)}(\mathbf{b}_\perp) + (\hat{b}^i\hat{\phi}^j + \hat{\phi}^i\hat{b}^j)v_T^{(m_s)}(\mathbf{b}_\perp). \tag{47}$$

Here, $\hat{b}$ and $\hat{\phi}$ are unit vectors in the radial and counterclockwise tangential directions, respectively. Note that each of the tensor structures except for the δ^{ij} accompanying $p_T^{(m_s)}(\mathbf{b}_\perp)$ is traceless, so $p_T^{(m_s)}(\mathbf{b}_\perp)$ can be understood as the isotropic pressure.

To obtain the functions p_T, s_T, and v_T, one can contract the comoving stress tensor with multiples of the associated tensors

$$p_T^{(m_s)}(\mathbf{b}_\perp) = \frac{1}{2}\delta_{ij}S_T^{ij}(\mathbf{b}_\perp, m_s), \tag{48a}$$

$$s_T^{(m_s)}(\mathbf{b}_\perp) = \left(\hat{b}^i\hat{b}^j - \frac{1}{2}\delta^{ij}\right)S_T^{ij}(\mathbf{b}_\perp, m_s), \tag{48b}$$

$$v_T^{(m_s)}(\mathbf{b}_\perp) = \frac{1}{2}(\hat{b}^i\hat{\phi}^j + \hat{\phi}^i\hat{b}^j)S_T^{ij}(\mathbf{b}_\perp, m_s). \tag{48c}$$

With some straightforward but tedious algebra, combining these equations with Eq. (46) yields

$$p_T^{(m_s)}(\mathbf{b}_\perp) = \frac{1}{2}\left\{\frac{\partial^2}{\partial b_\perp^2} + \frac{1}{b_\perp}\frac{\partial}{\partial b_\perp} + \frac{1}{b_\perp^2}\frac{\partial^2}{\partial \phi^2}\right\}\tilde{\mathcal{D}}_T^{(m_s)}(\mathbf{b}_\perp), \tag{49a}$$

$$s_T^{(m_s)}(\mathbf{b}_\perp) = \left\{-\frac{\partial^2}{\partial b_\perp^2} + \frac{1}{b_\perp}\frac{\partial}{\partial b_\perp} + \frac{1}{b_\perp^2}\frac{\partial^2}{\partial \phi^2}\right\}\tilde{\mathcal{D}}_T^{(m_s)}(\mathbf{b}_\perp), \tag{49b}$$

$$v_T^{(m_s)}(\mathbf{b}_\perp) = \left\{-\frac{1}{b_\perp}\frac{\partial}{\partial b_\perp} + \frac{1}{b_\perp^2}\right\}\frac{\partial}{\partial \phi}\tilde{\mathcal{D}}_T^{(m_s)}(\mathbf{b}_\perp). \tag{49c}$$

It will be helpful for numerical applications to have expressions for the functions p_T, s_T, and v_T in terms of Hankel transforms rather than coordinate derivatives. Some algebra and identities for Bessel functions can be used to accomplish this. We spare the reader the details of the derivation, stating only the results. For specific polarization states, these functions are given by

$$p_T^{(\pm 1)}(\mathbf{b}_\perp) = \frac{p^{(+)}(b_\perp) + p^{(0)}(b_\perp)}{2} \pm \sin\phi\, p_T^{\sin\phi}(b_\perp) + \frac{1}{2}\cos 2\phi\, p_T^{\cos 2\phi}(b_\perp), \tag{50a}$$

$$s_T^{(\pm 1)}(\mathbf{b}_\perp) = \frac{s^{(+)}(b_\perp) + s^{(0)}(b_\perp)}{2} \pm \sin\phi\, s_T^{\sin\phi}(b_\perp) + \frac{1}{2}\cos 2\phi\, s_T^{\cos 2\phi}(b_\perp), \tag{50b}$$

$$v_T^{(\pm 1)}(\mathbf{b}_\perp) = \cos\phi\, v_T^{\cos\phi}(b_\perp) + \frac{1}{2}\sin 2\phi\, v_T^{\sin 2\phi}(b_\perp), \tag{50c}$$

and for the $m_s = 0$ state are

$$p_T^{(0)}(\mathbf{b}_\perp) = p^{(+)}(b_\perp) - \cos 2\phi\, p_T^{\cos 2\phi}(b_\perp), \tag{50d}$$

$$s_T^{(0)}(\mathbf{b}_\perp) = s^{(+)}(b_\perp) - \cos 2\phi\, s_T^{\cos 2\phi}(b_\perp), \tag{50e}$$

$$v_T^{(0)}(\mathbf{b}_\perp) = -\sin 2\phi\, v_T^{\sin 2\phi}(b_\perp). \tag{50f}$$

The ϕ modulations in these functions are given by

$$p_T^{\sin\phi}(b_\perp) = \frac{1}{2\pi}\frac{1}{4P^+}\frac{1}{2M}\left\{-\frac{1}{2}\mathcal{H}_1[k^3\mathcal{D}_T^{\sin\phi}(-k^2)](b_\perp)\right\}, \tag{51a}$$

$$s_T^{\sin\phi}(b_\perp) = \frac{1}{2\pi}\frac{1}{4P^+}\frac{1}{2M}\{\mathcal{H}_1[k^3\mathcal{D}_T^{\sin\phi}(-k^2)](b_\perp) - \frac{2}{b_\perp}\mathcal{H}_2[k^2\mathcal{D}_T^{\sin\phi}(-k^2)](b_\perp)\}, \tag{51b}$$

$$v_T^{\cos\phi}(b_\perp) = \frac{1}{2\pi}\frac{1}{4P^+}\frac{1}{2M}\left\{\frac{1}{b_\perp}\mathcal{H}_2[k^2\mathcal{D}_T^{\sin\phi}(-k^2)](b_\perp)\right\}, \tag{51c}$$

and the 2ϕ modulations by

$$p_T^{\cos 2\phi}(b_\perp) = \frac{1}{2\pi}\frac{1}{4P^+}\frac{1}{4M^2}\left\{-\frac{1}{2}\mathcal{H}_2[k^4\mathcal{D}_T^{\cos 2\phi}(-k^2)](b_\perp)\right\}, \tag{51d}$$

$$s_T^{\cos 2\phi}(b_\perp) = \frac{1}{2\pi}\frac{1}{4P^+}\frac{1}{4M^2}\left\{-\frac{1}{2}\mathcal{H}_0[k^4\mathcal{D}_T^{\cos 2\phi}(-k^2)](b_\perp) - \frac{1}{2}\mathcal{H}_4[k^4\mathcal{D}_T^{\cos 2\phi}(-k^2)](b_\perp)\right\}, \tag{51e}$$

$$v_T^{\sin 2\phi}(b_\perp) = \frac{1}{2\pi}\frac{1}{4P^+}\frac{1}{4M^2}\left\{\frac{1}{4}\mathcal{H}_0[k^4\mathcal{D}_T^{\cos 2\phi}(-k^2)](b_\perp) - \frac{1}{4}\mathcal{H}_4[k^4\mathcal{D}_T^{\cos 2\phi}(-k^2)](b_\perp)\right\}. \tag{51f}$$

For transversely polarized states, the eigenpressures will no longer be radial and tangential. The eigenpressures are instead given by[2]

$$P_{T,\pm}^{(m_s)}(\mathbf{b}_\perp) = p_T^{(m_s)}(\mathbf{b}_\perp) \pm \sqrt{\frac{1}{4}(s_T^{(m_s)}(\mathbf{b}_\perp))^2 + (v_T^{(m_s)}(\mathbf{b}_\perp))^2}. \tag{52a}$$

These eigenpressures are normal stresses along ϕ-dependent unit vectors $\hat{e}_\pm$, whose angles with respect to the spin quantization axis $\mathbf{s}_\perp = \hat{x}$ are given by

$$\theta_\pm^{(m_s)}(\mathbf{b}_\perp) = \phi + \frac{1}{2}\tan^{-1}\left(\frac{2v_T^{(m_s)}(\mathbf{b}_\perp)}{s_T^{(m_s)}(\mathbf{b}_\perp)}\right) + \Theta(\pm s_T^{(m_s)}(\mathbf{b}_\perp))\frac{\pi}{2}, \tag{52b}$$

where $\Theta(x)$ is the Heaviside step function. The unit eigenvectors are then written

$$\hat{e}_\pm^{(m_s)}(\mathbf{b}_\perp) = \cos(\theta_\pm^{(m_s)}(\mathbf{b}_\perp))\hat{x} + \sin(\theta_\pm^{(m_s)}(\mathbf{b}_\perp))\hat{y}. \tag{52c}$$

It is also possible to categorize the eigenpressures in an alternative way

$$\bar{P}_{T,r}^{(m_s)}(\mathbf{b}_\perp) = p_T^{(m_s)}(\mathbf{b}_\perp) + \mathrm{sign}(s_T^{(m_s)}(\mathbf{b}_\perp))\sqrt{\frac{1}{4}(s_T^{(m_s)}(\mathbf{b}_\perp))^2 + (v_T^{(m_s)}(\mathbf{b}_\perp))^2}, \tag{53a}$$

$$\bar{P}_{T,t}^{(m_s)}(\mathbf{b}_\perp) = p_T^{(m_s)}(\mathbf{b}_\perp) - \mathrm{sign}(s_T^{(m_s)}(\mathbf{b}_\perp))\sqrt{\frac{1}{4}(s_T^{(m_s)}(\mathbf{b}_\perp))^2 + (v_T^{(m_s)}(\mathbf{b}_\perp))^2}, \tag{53b}$$

whose angles with respect to the spin quantization axis are

$$\bar{\theta}_r^{(m_s)}(\mathbf{b}_\perp) = \phi + \frac{1}{2}\tan^{-1}\left(\frac{2v_T^{(m_s)}(\mathbf{b}_\perp)}{s_T^{(m_s)}(\mathbf{b}_\perp)}\right), \tag{53c}$$

$$\bar{\theta}_t^{(m_s)}(\mathbf{b}_\perp) = \phi + \frac{1}{2}\tan^{-1}\left(\frac{2v_T^{(m_s)}(\mathbf{b}_\perp)}{s_T^{(m_s)}(\mathbf{b}_\perp)}\right) + \frac{\pi}{2}. \tag{53d}$$

At every $\mathbf{b}_\perp$, these of course furnish the same pair of eigenvectors and eigenvalues as Eq. (52); the difference lies in how the pairs are sorted into $\mathbf{b}_\perp$-dependent functions. The eigenvalue/eigenvector pairs in Eq. (53) in particular reduce to the familiar radial and tangential eigenpressures in the helicity case (where $v_T = 0$). However, there is benefit to using Eq. (52) instead of Eq. (53) for transversely polarized states; namely, that when $v_T \neq 0$, only the former are continuous across $s_T = 0$. This can be seen both in the square root function in the pressure functions themselves, and in how the step function in the angle functions compensates the $\frac{\pi}{2}$ discontinuity between $\frac{1}{2}\tan^{-1}(\infty)$ and between $\frac{1}{2}\tan^{-1}(-\infty)$.

2. Mechanical radius

It has been hypothesized [12,13,27,30] that the radial pressure is a positive-definite quantity for stable systems, and can thus be used to define a positive-definite "mechanical radius" that gives an estimate of a hadron's size

$$\langle b_\perp^2\rangle_{\mathrm{mech}} = \frac{\int \mathrm{d}^2\mathbf{b}_\perp \mathbf{b}_\perp^2 p_r(\mathbf{b}_\perp)}{\int \mathrm{d}^2\mathbf{b}_\perp p_r(\mathbf{b}_\perp)}. \tag{54}$$

[2]A capital P is used to signify transverse eigenpressures to assist visually distingiushing them from other auxilliary functions such as $p_T^{(m_s)}$.

For transversely polarized states the radial pressure is not an eigenpressure, but it is nevertheless a normal stress along the $\hat{b}$ direction, and is given by

$$p_{\mathrm{Tr}}^{(m_s)}(\mathbf{b}_\perp) = \frac{1}{b_\perp}\frac{\partial \tilde{\mathcal{D}}_T^{(m_s)}(\mathbf{b}_\perp)}{\partial b_\perp} + \frac{\partial^2 \tilde{\mathcal{D}}_T^{(m_s)}(\mathbf{b}_\perp)}{\partial \phi^2}. \quad (55)$$

In both the numerator and denominator, the integrals over the azimuthal modulations become zero. Thus, for either helicity or transversely polarized states, the numerator becomes, via integration by parts,

$$\int \mathrm{d}^2\mathbf{b}_\perp \mathbf{b}_\perp^2 p_r(\mathbf{b}_\perp) = -\frac{1}{2P^+}\mathcal{D}(0). \quad (56)$$

The denominator, with a little integration calculus, can be shown to be

$$\int \mathrm{d}^2\mathbf{b}_\perp p_r(\mathbf{b}_\perp) = -\frac{1}{16\pi P^+}\int_{-\infty}^0 \mathrm{d}t \int_0^{2\pi} \mathrm{d}\phi \mathcal{D}(\boldsymbol{\Delta}_\perp), \quad (57)$$

where the modulations again integrate to zero. The mechanical radius is thus given by

$$\langle b_\perp^2\rangle_{\mathrm{mech}} = \left.\frac{4\mathcal{D}(0)}{\int_{-\infty}^0 \mathrm{d}t\mathcal{D}(t)}\right|_{\sin\phi=0,\cos 2\phi=0}. \quad (58)$$

For specific helicity states of massive hadrons, we have

$$\langle b_\perp^2\rangle_{\mathrm{mech}}(\lambda=\pm 1) = \frac{4(\mathcal{G}_3(0)-\mathcal{G}_6(0))}{\int_{-\infty}^0 \mathrm{d}t(\mathcal{G}_3(t)-\mathcal{G}_6(t))}, \quad (59a)$$

$$\langle b_\perp^2\rangle_{\mathrm{mech}}(\lambda=0) = \frac{4\mathcal{G}_3(0)}{\int_{-\infty}^0 \mathrm{d}t\mathcal{G}_3(t)}, \quad (59b)$$

while for specific transverse-polarization states, we have

$$\langle b_\perp^2\rangle_{\mathrm{mech},T}(m_s=\pm 1) = \frac{4(\mathcal{G}_3(0)-\frac{1}{2}\mathcal{G}_6(0))}{\int_{-\infty}^0 \mathrm{d}t(\mathcal{G}_3(t)-\frac{1}{2}\mathcal{G}_6(t))}, \quad (59c)$$

$$\langle b_\perp^2\rangle_{\mathrm{mech},T}(m_s=0) = \frac{4(\mathcal{G}_3(0)-\mathcal{G}_6(0))}{\int_{-\infty}^0 \mathrm{d}t(\mathcal{G}_3(t)-\mathcal{G}_6(t))}. \quad (59d)$$

For the unpolarized state, the numerator and denominator need to be averaged separately. The unpolarized mechanical radius of a massive hadron is given by

$$\overline{\langle b_\perp^2\rangle_{\mathrm{mech}}} = \frac{4(\mathcal{G}_3(0)-\frac{2}{3}\mathcal{G}_6(0))}{\int_{-\infty}^0 \mathrm{d}t(\mathcal{G}_3(t)-\frac{2}{3}\mathcal{G}_6(t))}. \quad (60)$$

IV. NUMERICAL ILLUSTRATION

As a simple numerical illustration, we present light front densities for the deuteron in a light cone convolution model [43–46]. The model provides a description of deuteron structure in terms of on-shell nucleons, which allows for on-shell gravitational form factors to be used for the nucleon, according to the standard formulas (e.g., Eq. (6) of Ref. [13]).

A potential downside of the light cone model is that it breaks manifest Lorentz covariance by truncating the Fock state at a two-nucleon state—a truncation that is invariant under the kinematic subgroup, but not under dynamical transformations. The form factor and helicity amplitude breakdowns in Eqs. (1) and (2) are a consequence of Lorentz covariance, and accordingly, the helicity amplitudes calculated in this model through different components of the EMT may be inconsistent. (Compare to Refs. [43,45], where polynomiality breaks down for generalized parton distributions of the deuteron, which makes extraction of the GFFs ambiguous.) Additionally, the components T^{+i} and T^{ij} are "bad" components [47,48], in the sense that they mix Fock states with different numbers of particles, and the truncation of the deuteron Fock state at two nucleons accordingly drops potentially relevant physics.

Despite this potential shortcoming, we adopt the model in question, largely due to the lack of alternatives with the desirable covariance property. Moreover, this section is primarily meant to illustrate the general formalism developed above—a purpose for which the model is perfectly adequate. To deal with the issue of inconsistent helicity amplitudes, we consider specifically components of the EMT that give expected behavior of the GFFs at $t=0$, namely that the $t=0$ results for all helicity transitions are zero [e.g., $\mathcal{J}_{+0}(0)=0$], and that $\mathcal{D}_{\lambda\lambda'}(0)$ is finite for all λ and λ'.

We calculate in a frame where $\mathbf{P}_\perp = 0$. We have $\Delta^+ = 0$ by construction, and it also follows that $\Delta^- = 0$. Without loss of generality, we can consider $\Delta^x = \sqrt{-t}$ and $\Delta^y = 0$. In the convolution the momentum of the "active" nucleon enters the matrix element of the EMT. This has the same Δ^+ and $\Delta_\perp$ as for the deuteron, whereas Δ^- does not enter into the relevant matrix elements.

We find the following EMT matrix elements to provide GFFs with the required $t=0$ behavior

$$\frac{1}{2(P^+)^2}\langle p'\lambda'|T^{++}|p\lambda\rangle = \mathcal{A}_{\lambda'\lambda}(t), \quad (61a)$$

$$-\frac{1}{P^+\sqrt{-t}}\langle p'\lambda'|T^{+R}|p\lambda\rangle = \mathcal{J}_{\lambda'\lambda}(t), \quad (61b)$$

$$-2\langle p'\lambda'|T^{RR}|p\lambda\rangle = t\mathcal{D}_{\lambda'\lambda}, \quad (61c)$$

where the R and L components are defined via

$$a^R = a^x + ia^y, \quad (62a)$$

$$a^L = a^x - ia^y. \quad (62b)$$

These allow us to calculate the necessary helicity amplitudes directly. Specifically, off-diagonal matrix elements contribute to the $\sin\phi$ (one unit helicity difference) and $\cos 2\phi$ (two units) modulations for the transversely polarized states.

Because of Lorentz covariance violations by the convolution model, several symmetry relations laid out in Appendix B are violated by applying Eq. (61) to the model. For instance, we find $\mathcal{J}_{+0}(t) \neq -\mathcal{J}^*_{0+}(t)$. In this case specifically, we find $\mathcal{J}_{+0}(0) = 0$ but $\mathcal{J}_{0+}(0) \neq 0$. Since physically this helicity amplitude should vanish at $t = 0$, we use Eq. (61) to calculate $\mathcal{J}_{+0}(t)$ specifically, and then set $\mathcal{J}_{0+}(t) = -\mathcal{J}^*_{+0}(t)$. (If we use T^{+L} rather than T^{+R} to calculate these same helicity amplitudes, their behavior is actually reversed. This behavior reversal is an inevitable consequence of stricter symmetry properties than Lorentz covariance, namely hermiticity and parity invariance.) In all cases where the relations in Appendix B are violated, we restore the relations by fiat and use Eq. (61) to calculate the specific helicity amplitude with the required $t = 0$ behavior.

To proceed, we also need the following matrix elements for the nucleon light front EMT, obtained by evaluating Eq. (27) of Ref. [30]. For T^{++} matrix elements

$$\frac{1}{2(P^+)^2}\langle p'_N\lambda|T^{++}|p_N\lambda\rangle = \left(\frac{\alpha_N}{2}\right)^2 A(t), \tag{63a}$$

$$\frac{1}{2(P^+)^2}\langle p'_N-|T^{++}|p_N+\rangle = -\left(\frac{\alpha_N}{2}\right)^2 \frac{\sqrt{-t}}{2M}[A(t)-2J(t)], \tag{63b}$$

$$\frac{1}{2(P^+)^2}\langle p'_N+|T^{++}|p_N-\rangle = \left(\frac{\alpha_N}{2}\right)^2 \frac{\sqrt{-t}}{2M}[A(t)-2J(t)], \tag{63c}$$

for T^{+R} matrix elements,

$$-\frac{1}{P^+\sqrt{-t}}\langle p'_N\lambda|T^{+R}|p_N\lambda\rangle = \frac{\alpha_N}{2}\left(-2\frac{P^R_N}{\sqrt{-t}}A(t)+\lambda J(t)\right), \tag{64a}$$

$$-\frac{1}{P^+\sqrt{-t}}\langle p'_N-|T^{+R}|p_N+\rangle = \frac{\alpha_N}{2}\frac{P^R_N}{M}[A(t)-2J(t)], \tag{64b}$$

$$\begin{aligned}&-\frac{1}{P^+\sqrt{-t}}\langle p'_N+|T^{+R}|p_N-\rangle\\ &= -\frac{\alpha_N}{2}\frac{P^R_N}{M}\left[A(t)+\left(\frac{P^L_N}{P^R_N}-1\right)J(t)\right],\end{aligned} \tag{64c}$$

and for T^{RR} matrix elements,

$$2\langle p'_N\lambda|T^{RR}|p_N\lambda\rangle = 4(P^R_N)^2A(t) - tD(t) - 2\lambda\sqrt{-t}P^R_N J(t), \tag{65a}$$

$$\begin{aligned}2\langle p'_N-|T^{RR}|p_N+\rangle &= -\frac{\sqrt{-t}}{2M}[4(P^R_N)^2A(t)-tD(t)]\\ &\quad + 2\frac{\sqrt{-t}}{M}(P^R_N)^2J(t),\end{aligned} \tag{65b}$$

$$\begin{aligned}2\langle p'_N+|T^{RR}|p_N-\rangle &= \frac{\sqrt{-t}}{2M}[4(P^R_N)^2A(t)-tD(t)]\\ &\quad + 2\frac{\sqrt{-t}}{M}P^R_N P^L_N J(t).\end{aligned} \tag{65c}$$

Here, α_N is related to the light front momentum fraction of the active nucleon,

$$\alpha_N = \frac{2p^+_N}{p^+} = \frac{2p'^+_N}{p^+}. \tag{66}$$

For the nucleon form factors, we use simple multipole parametrizations, motivated by the investigations of Ref. [49] (see Sec. V.C thereof in particular),

$$A(t) = 2J(t) = \frac{1}{(1-t/m^2_{f_2(1270)})(1-t/m^2_{f_2(1430)})}, \tag{67a}$$

$$D(t) = \frac{D(0)}{(1-t/m^2_{f_2(1270)})(1-t/m^2_{f_2(1430)})(1-t/m^2_{\sigma(800)})}, \tag{67b}$$

with $D(0) = -2$, motivated by lattice QCD findings [50].

The helicity amplitudes in this model are presented in Fig. 1. From these, a variety of light front densities can be obtained. We present a selected sample of these densities, in order to not take up too much space. In particular, p^+ densities can be calculated using Eqs. (16a) and (20), and the pressure distributions using Eqs. (43), (50), (51), and (52).

First, in Fig. 2, we present light front momentum (p^+) densities for both $\lambda = 0$ and $\lambda = +1$ helicity states, as well as for the $m_s = 0$ and $m_s = +1$ transversely polarized states. The p^+ densities obtained from this model are especially robust, since they are obtained through the "good" component T^{++} of the EMT. They also provide the clearest, most transparent description of the deuteron's structure.

A curious aspect of the $m_s = +1$ state is its deformation towards the $+y$ direction. This is a peculiarity of the use of light front coordinates, and has been noticed for the deuteron's electric charge density previously in Ref. [38,42], as well as in both the charge density [25] and p^+ density [51] of a transversely polarized proton. In Ref. [25], this deformation was interpreted in terms of

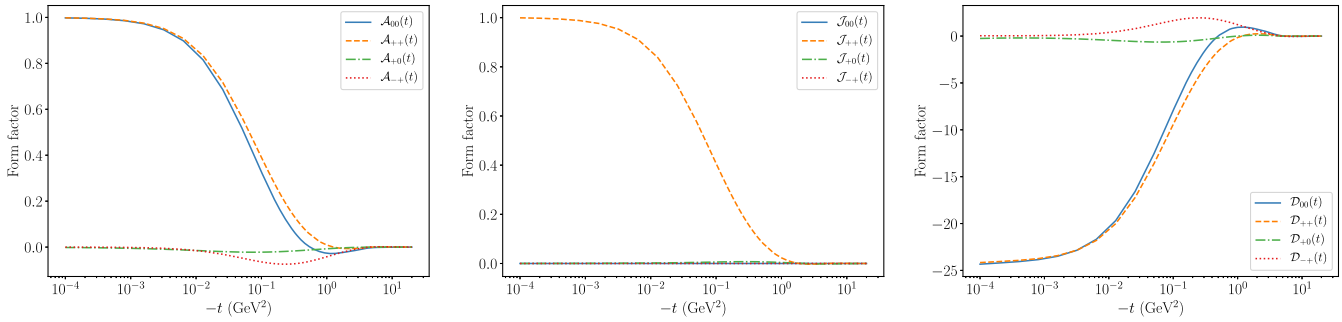

FIG. 1. The helicity amplitudes $\mathcal{A}(t)$, $\mathcal{J}(t)$ and $\mathcal{D}(t)$ of the deuteron for various helicity combinations. Those not explicitly given in the plots are determined from these using the relations in Appendix B.

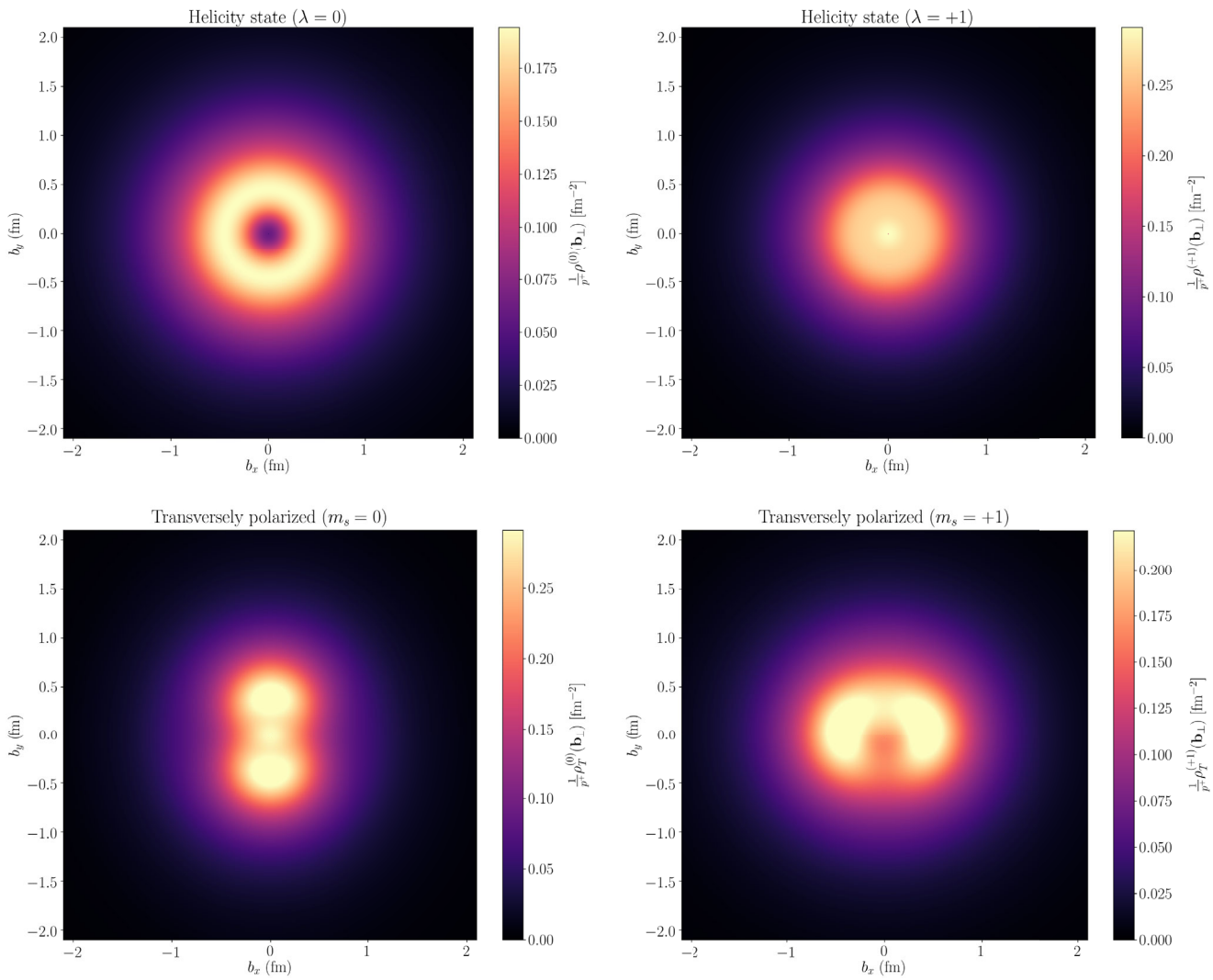

FIG. 2. The p^+ density of the deuteron in various polarization states, with p^+ divided out to provide a boost-invariant density that is normalized to 1. A left-handed coordinate system is used, so that the z direction is into rather than out of the page. The panels are (top-left) helicity state with $\lambda = 0$, (top-right) helicity state with $\lambda = +1$, (bottom-left) transverse polarization along x axis with $m_s = 0$, and (bottom-right) transverse polarization along x axis with $m_s = +1$.

distortions created by the point of view of an observer moving quickly towards the target. However, no such reference frame has actually been chosen here.

The transverse deformations are likely due to a mix of different effects, including the use of fixed x^+ rather than fixed x^0, the fact that x^- has been integrated out, and that we are considering a density of P^+ rather than a density of P^0. Note that there is more P^3 on one side of the axis of rotation than the other, since the axis of rotation is along the x axis, and modulations in the P^3 density would be present in the P^+ density as well, even in a three-dimensional instant form density in the rest frame. There may also be modulation effects from Wigner-Melosh rotations connecting states with light front spin and canonical spin, as was observed in Refs. [29,42,52] for spin-half systems.

Let us consider the static quantities associated with the momentum densities. Starting with the radii, using Eq. (32), we find the following radii for helicity states

$$\langle b_\perp \rangle_{p^+}(\lambda = 0) = 1.77 \text{ fm}, \tag{68a}$$

$$\langle b_\perp \rangle_{p^+}(\lambda = 0) = 1.69 \text{ fm}, \tag{68b}$$

$$\overline{\langle b_\perp \rangle_{p^+}} = 1.72 \text{ fm}. \tag{68c}$$

These results are roughly compatible with the known charge radius of the deuteron. The Breit frame deuteron charge radius is 2.130 fm [53], which scaled down by $\sqrt{2/3}$ to give a rough estimate for a 2D charge radius, gives 1.739 fm.

For the transversely polarized states, we can calculate a quadrupole moment. Using Eqs. (30) and (B3), the light front quadrupole moment is found to be

$$\mathcal{Q}_{\text{LF}} = 4\lim_{t\to 0}\frac{\mathcal{A}_{-+}(t)}{t} = 0.27 p^+\text{-fm}, \tag{69}$$

which is surprisingly close to the empirical value of the electric quadrupole moment, $0.2859e$-fm [54–56].

The pressure distributions are of special interest, due to the amount of attention these have received in the hadron physics community recently. Unfortunately, the light cone convolution model is less trustworthy for these quantities because they correspond to "bad" components of the EMT, namely, T^{ij}. An ideal situation would be to obtain $\mathcal{D}_{\lambda\lambda'}(t)$ from a manifestly covariant model. Nonetheless, for illustration of the formalism, we present the pressure distributions obtained from this model.

A selection of eigenpressures are presented in Fig. 3, with the selection limited to save space. For helicity states, the radial pressure is selected, and for transversely polarized states, the "+" eigenpressure is selected according to Eq. (52). The color is selected to show magnitude and sign of the pressure, and two-sided arrows to signify direction.

We feel it is important to reiterate the physical meaning of intrinsic pressure and its sign in this context, as was explained previously in Ref. [51]. Since the deuteron is in equilibrium, the expectation value of the force acting over any region of the transverse plane is exactly zero. By Gauss's theorem, this means that the integral of $\mathbf{F}_\perp \cdot \hat{n}$ over the surface of any region must be zero. The stresses encoded by the expectation value of T^{ij} correspond to forces acting on this region from all directions, which sum to a net force of zero. A positive pressure therefore does *not* indicate a net repulsive force from the center, nor does a negative pressure signify a confining force towards the center, as was claimed in Ref. [57]. A positive pressure means that particles in this region of space are experiencing pushing forces *from both directions*, and a negative pressure likewise means they are experiencing pulling forces *from both directions*. For the radial eigenpressures (helicity states), these directions are towards and away from the center of the deuteron, while for transversely polarized states, the directions are indicated by white arrows overlaid on the plot.

In fact, since the densities obtained in this formalism correspond to stresses seen by transversely comoving observers, the pressures are *static* pressures or *intrinsic* pressures, and should be contrasted by *dynamic* pressures which include impulse imparted by flow or motion of the medium (see for instance Chapter 4-3 of Ref. [58]).

It has been postulated throughout the literature [13,27,30] that the radial pressure should be positive as a stability condition. Our result for the $\lambda = 0$ radial pressure, in the top-left panel of Fig. 3, violates this expectation. Although the stability requirement is merely a conjecture lacking proof, it is premature to declare our model result to be a counter-example, owing to the possible shortcomings of a light cone convolution model. For now, we consider the results here to be tentative and open to replacement by results from a manifestly covariant calculation.

If we do however take the results in Fig. 3 at face value, they paint an interesting picture of the dynamics at play within the deuteron. There appears to be a ring of roughly half a femtometer at which pressure is more intense. Within this ring, near the center, the pressure becomes negative for the helicity zero state—specifically in the region where the p^+ density is depleted (see Fig. 2). The exact meaning of this negative pressure (and its reality, given limitations of the model) is unclear. One possibility is that the negative pressure corresponds to attractive forces pulling particles inside the ring towards the ring, and that the pressure remains negative because the pressure exerted by other particles crowding the area is not present.

Let us consider static quantities associated with the comoving stress tensor. First of all, the static D-terms for helicity states are

$$\mathcal{D}_0(0) = -24.33, \tag{70a}$$

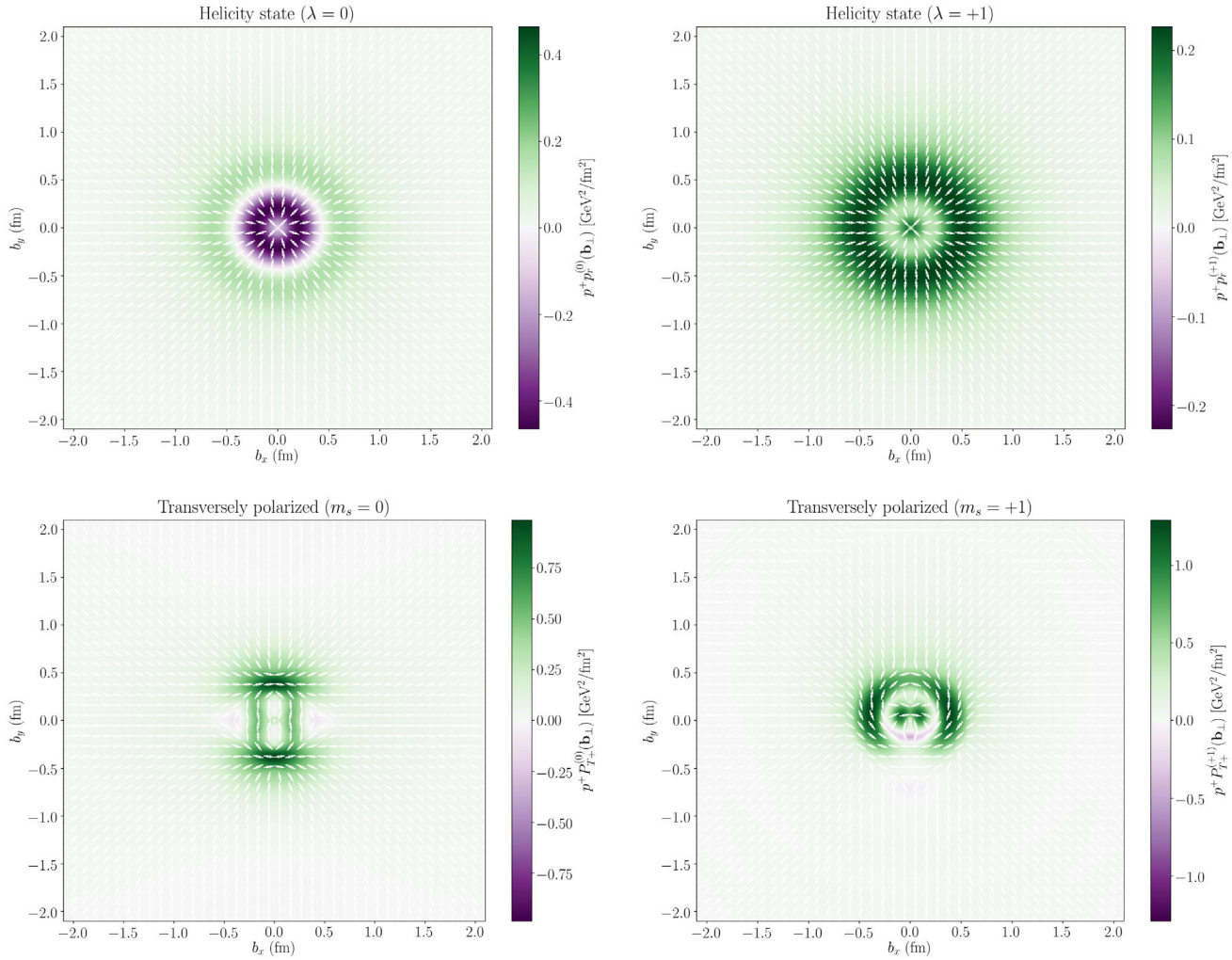

FIG. 3. The radial (or +) eigenpressure of the deuteron in various polarization states, multiplied by p^+ to provide a boost-invariant density. See Eq. (52) and the discussion around it for an explanation of the eigenpressures. The arrows indicate directions in which the pressure is acting, and are double-sided because pressures from both directions act with the same magnitude and result in a net zero force (see text for further elaboration). A left-handed coordinate system is used, so that the z direction is into rather than out of the page. The panels are (top-left) helicity state with $\lambda = 0$, (top-right) helicity state with $\lambda = +1$, (bottom-left) transverse polarization along x axis with $m_s = 0$, and (bottom-right) transverse polarization along x axis with $m_s = +1$.

$$\mathcal{D}_{\pm 1}(0) = -24.16. \tag{70b}$$

These values are large, negative, and nearly identical. It is worth noting that negativity of $\mathcal{D}(0)$ has been frequently postulated [12,13,27,30] as a *looser* stability criterion than the radial pressure being positive, and that our deuteron model at least satisfies this condition. Next, we consider mechanical radii calculated according to Eq. (58),

$$\langle b_\perp \rangle_{\text{mech}}(\lambda = 0) = 2.39 \text{ fm}, \tag{71a}$$

$$\langle b_\perp \rangle_{\text{mech}}(\lambda = +1) = 1.06 \text{ fm}, \tag{71b}$$

$$\overline{\langle b_\perp \rangle_{\text{mech}}} = 1.24 \text{ fm}. \tag{71c}$$

These results are surprising. It is worth stressing, as discussed above, that the "average" involves averaging the numerator and denominator separately, rather than taking the mean of the three radii; this is why the average mechanical radius is not close to the mean of the three polarization states' radii. In any case, the disparity between the radii is stark, and can be understood clearly by looking at Fig. 3; the negative presssure near the center of the helicity-zero state greatly enhances its mechanical radius.

V. SUMMARY AND OUTLOOK

In this work, we obtained the two-dimensional light front densities of momentum, angular momentum, and pressures within spin-one targets. In contrast to the spin-half case, the densities have helicity dependence, and the densities of

transversely polarized spin-one hadrons can exhibit quadrupole deformations that are related to the differences between the helicity-one and helicity-zero densities. All of these special properties of spin-one light front densities have been illustrated with a light front convolution model of the deuteron.

Experimentally, the spatial densities for the deuteron could be extracted from data for coherent hard exclusive reactions on the deuteron. These are challenging measurements, however, due to the steeper t-slopes of the coherent deuteron cross section compared to that of the nucleon. Current data is scarce: the HERMES Collaboration has measured deeply virtual Compton scattering (DVCS) on the deuteron with both unpolarized [59] and polarized targets [60], and Jefferson Lab (JLab) has more recent results for coherent π^0 electroproduction on the deuteron [61]. In the future, more data should be forthcoming from JLab [62,63], and especially the future electron-ion collider [64,65] with its dedicated far-forward detectors setup. Accessing the gravitational form factors from these data is a nontrivial inverse problem, as they are related to Mellin moments of twist-2 vector generalized parton distributions (GPDs) [17], which are present in the amplitudes in the Compton form factors, being x-convolutions of the GPDs with a hard scattering coefficient.

In a following companion paper [34], we apply the formalism developed here to the photon as a special case. A few minor modifications are made to accommodate the massless case, but these result in simplifications of the formalism. The photon is an especially pertinent target to consider, since the employment of a light front formalism allows for its densities to be calculated.

ACKNOWLEDGMENTS

The authors would like to thank Ian Cloët and Gerald Miller for enlightening discussions that helped contribute to this work. A. F. was supported by the U.S. Department of Energy Office of Science, Office of Nuclear Physics under Award No. DE-FG02-97ER-41014. W. C. was supported by the National Science Foundation under Award No. 2111442.

APPENDIX A: LIGHT FRONT SPIN-ONE POLARIZATION VECTORS

This appendix uses the polarization vectors from Refs. [37,43,45], but at $\xi = 0$, which is the case relevant to local operators such as the EMT. Note that $\Delta^+ = -2\xi P^+$, so having $\xi = 0$ is equivalent to having $\Delta^+ = 0$, and we take $\Delta^+ = (n \cdot \Delta) = 0$ throughout the paper (including this appendix).

The polarization basis vectors are given explicitly by

$$\varepsilon_0^\mu = \frac{1}{M}\left(p^\mu - M^2 \frac{n^\mu}{(P \cdot n)}\right), \tag{A1}$$

$$\varepsilon_0'^\mu = \frac{1}{M}\left(p'^\mu - M^2 \frac{n^\mu}{(P \cdot n)}\right), \tag{A2}$$

$$\varepsilon_1^\mu = \frac{1}{\sqrt{-t}}\left(\Delta^\mu + t\frac{n^\mu}{2(P \cdot n)}\right), \tag{A3}$$

$$\varepsilon_1'^\mu = \frac{1}{\sqrt{-t}}\left(\Delta^\mu - t\frac{n^\mu}{2(P \cdot n)}\right), \tag{A4}$$

$$\varepsilon_2^\mu = \varepsilon_2'^\mu = -\frac{1}{\sqrt{-t}}\frac{\epsilon^\mu_{\nu\alpha\beta}P^\nu \Delta^\alpha n^\beta}{(P \cdot n)}, \tag{A5}$$

where the Levi-Civita symbol is normalized to satisfy $\varepsilon^{0123} = +1$. These polarization basis vectors satisfy the following orthogonality and normalization relations,

$$\varepsilon_i \cdot \varepsilon_j = \varepsilon_i' \cdot \varepsilon_j' = -\delta_{ij}, \tag{A6}$$

$$\varepsilon_i \cdot p = \varepsilon_i' \cdot p' = 0. \tag{A7}$$

The positive and negative helicity vectors are defined via [45][3]

$$\varepsilon_\pm = \mp\, e^{\pm i\phi_\Delta}\frac{\varepsilon_1 \pm i\varepsilon_2}{\sqrt{2}}, \tag{A8}$$

and equivalently for the primed four-vectors, where ϕ_Δ is the azimuthal angle of the momentum transfer $\mathbf{\Delta}_\perp$ with respect to a fixed $\hat{x}$ axis. The positive and negative helicity vectors satisfy

$$\varepsilon_+^* \cdot \varepsilon_+ = \varepsilon_-'^* \cdot \varepsilon_-' = -1, \tag{A9}$$

$$\varepsilon_+^* \cdot \varepsilon_- = \varepsilon_-'^* \cdot \varepsilon_+' = 0, \tag{A10}$$

$$\varepsilon_0 \cdot p = \varepsilon_+ \cdot p = \varepsilon_- \cdot p = 0, \tag{A11}$$

$$\varepsilon_0' \cdot p' = \varepsilon_+' \cdot p' = \varepsilon_-' \cdot p' = 0. \tag{A12}$$

For $\varepsilon_\pm$ (and their primed counterparts) specifically,

$$\varepsilon_+ \cdot n = \varepsilon_+' \cdot n = \varepsilon_- \cdot n = \varepsilon_-' \cdot n = 0. \tag{A13}$$

For massless spin-one particles such as the photon, using $\varepsilon_\pm$ as the polarization vectors thus amounts to using light cone gauge.

Several helpful explicit four-products include

$$(\varepsilon_0 \cdot \Delta) = \frac{-t}{2M}, \tag{A14}$$

[3]Note that Refs. [37,43] take $\phi_\Delta = \pi$ and define $\epsilon_1^\mu, \epsilon_2^\mu$ (and primed equivalent vectors) with an opposite sign.

$$(\varepsilon_0' \cdot \Delta) = \frac{+t}{2M}, \tag{A15}$$

$$(\varepsilon_1 \cdot \Delta) = (\varepsilon_1' \cdot \Delta) = -\sqrt{-t}, \tag{A16}$$

$$(\varepsilon_2 \cdot \Delta) = (\varepsilon_2' \cdot \Delta) = 0, \tag{A17}$$

and several explicit outer products include

$$\frac{1}{2}\varepsilon_0^{\{\mu}\varepsilon_0'^{\nu\}} = \frac{1}{M^2}\left(P^\mu P^\nu - \frac{1}{4}\Delta^\mu\Delta^\nu\right) - \frac{n^{\{\mu}P^{\nu\}}}{(P\cdot n)} + \frac{M^2 n^\mu n^\nu}{(P\cdot n)^2}, \tag{A18}$$

$$\frac{1}{2}\varepsilon_1^{\{\mu}\varepsilon_1'^{\nu\}} = -\frac{\Delta^\mu\Delta^\nu}{t} + \frac{t}{4}\frac{n^\mu n^\nu}{(P\cdot n)^2}, \tag{A19}$$

$$\frac{1}{2}\varepsilon_2^{\{\mu}\varepsilon_2'^{\nu\}} = -g^{\mu\nu} - \left(1 - \frac{t}{4M^2}\right)\frac{M^2 n^\mu n^\nu}{(P\cdot n)^2} + \frac{n^{\{\mu}P^{\nu\}}}{(P\cdot n)} + \frac{\Delta^\mu\Delta^\nu}{t}. \tag{A20}$$

APPENDIX B: EXPLICIT EMT MATRIX ELEMENTS

In this appendix we give explicit evaluations of all the helicity amplitudes in Eq. (2) in terms of the $\mathcal{G}_{1-6}(t)$ form factors in Eq. (1), using all combinations of the polarization vectors in Appendix A.

Firstly, for the $\mathcal{A}$ results:

$$\mathcal{A}_{00} = \left(1 + \frac{t}{2M^2}\right)\mathcal{G}_1(t) - \frac{t}{4M^2}(2\mathcal{G}_5(t) + \mathcal{G}_6(t)) - \frac{t^2}{8M^4}\mathcal{G}_2(t), \tag{B1}$$

$$\mathcal{A}_{++} = \mathcal{A}_{--} = \mathcal{G}_1(t) - \frac{t}{4M^2}\mathcal{G}_2(t), \tag{B2}$$

$$\mathcal{A}_{0+} = \mathcal{A}_{-0} = -\mathcal{A}_{+0}^* = -\mathcal{A}_{0-}^* = -\frac{\sqrt{-t}}{\sqrt{2}M}\left\{\mathcal{G}_1(t) - \frac{1}{2}\mathcal{G}_5(t) - \frac{t}{4M^2}\mathcal{G}_2(t)\right\}e^{i\phi_\Delta}, \tag{B3}$$

$$\mathcal{A}_{-+} = \mathcal{A}_{+-}^* = \frac{t}{4M^2}\mathcal{G}_2(t)e^{2i\phi_\Delta}. \tag{B4}$$

Next, for $\mathcal{J}(t)$:

$$\mathcal{J}_{00} = 0, \tag{B5}$$

$$\mathcal{J}_{++} = -\mathcal{J}_{--} = \frac{1}{2}\mathcal{G}_5(t), \tag{B6}$$

$$\mathcal{J}_{0+} = -\mathcal{J}_{-0} = -\mathcal{J}_{+0}^* = \mathcal{J}_{0-}^* = -\frac{\sqrt{-t}}{4\sqrt{2}M} \times \{\mathcal{G}_5(t) + \mathcal{G}_6(t)\}e^{i\phi_\Delta}, \tag{B7}$$

$$\mathcal{J}_{-+} = \mathcal{J}_{+-}^* = 0. \tag{B8}$$

Next, for $\mathcal{D}(t)$:

$$\mathcal{D}_{00} = \left(1 + \frac{t}{2M^2}\right)\mathcal{G}_3(t) - \frac{t}{4M^2}\mathcal{G}_6(t) - \frac{t^2}{8M^2}\mathcal{G}_4(t), \tag{B9}$$

$$\mathcal{D}_{++} = \mathcal{D}_{--} = \mathcal{G}_3(t) - \mathcal{G}_6(t) - \frac{t}{4M^2}\mathcal{G}_4(t), \tag{B10}$$

$$\mathcal{D}_{0+} = \mathcal{D}_{-0} = -\mathcal{D}_{+0}^* = -\mathcal{D}_{0-}^* = -\frac{\sqrt{-t}}{\sqrt{2}M}\left\{\mathcal{G}_3(t) - \frac{1}{2}\mathcal{G}_6(t) - \frac{t}{4M^2}\mathcal{G}_4(t)\right\}e^{i\phi_\Delta}, \tag{B11}$$

$$\mathcal{D}_{-+} = \mathcal{D}_{+-}^* = \frac{t}{4M^2}\mathcal{G}_4(t)e^{2i\phi_\Delta}. \tag{B12}$$

Next, for $\mathcal{E}(t)$:

$$\mathcal{E}_{00} = \frac{t}{2}(\mathcal{G}_5(t) + \mathcal{G}_6(t)), \tag{B13}$$

$$\mathcal{E}_{++} = \mathcal{E}_{--} = \frac{t}{4}(\mathcal{G}_5(t) - \mathcal{G}_6(t)), \tag{B14}$$

$$\mathcal{E}_{0+} = \mathcal{E}_{-0} = -\mathcal{E}_{+0}^* = -\mathcal{E}_{0-}^* = -\frac{\sqrt{-t}M}{2\sqrt{2}}\left\{\left(1 + \frac{t}{4M^2}\right)\mathcal{G}_5(t) + \frac{t}{4M^2}\mathcal{G}_6(t)\right\}e^{i\phi_\Delta}, \tag{B15}$$

$$\mathcal{E}_{-+} = \mathcal{E}_{+-}^* = -\frac{t}{4}(\mathcal{G}_5(t) + \mathcal{G}_6(t))e^{2i\phi_\Delta}. \tag{B16}$$

Next, for $\mathcal{H}(t)$:

$$\mathcal{H}_{00} = -\frac{tM^2}{2}\mathcal{G}_6(t), \tag{B17}$$

$$\mathcal{H}_{++} = \mathcal{H}_{--} = \frac{tM^2}{4}\left(1 - \frac{t}{2M^2}\right)\mathcal{G}_6(t), \tag{B18}$$

$$\mathcal{H}_{0+} = \mathcal{H}_{-0} = -\mathcal{H}_{+0}^* = -\mathcal{H}_{0-}^* = \frac{t\sqrt{-t}M}{4\sqrt{2}}\mathcal{G}_6(t)e^{i\phi_\Delta}, \tag{B19}$$

$$\mathcal{H}_{-+} = \mathcal{H}_{+-}^* = \frac{tM^2}{4}\mathcal{G}_6(t)e^{2i\phi_\Delta}. \tag{B20}$$

Lastly, for $\mathcal{K}(t)$:

$$\mathcal{K}_{00} = 0, \tag{B21}$$

$$\mathcal{K}_{++} = -\mathcal{K}_{--} = \frac{t}{8}\mathcal{G}_6(t), \tag{B22}$$

$$\mathcal{K}_{0+} = \mathcal{K}_{-0} = -\mathcal{K}^*_{+0} = -\mathcal{K}^*_{0-} = -\frac{\sqrt{-t}M}{4\sqrt{2}}\mathcal{G}_6(t)e^{i\phi_\Delta}, \tag{B23}$$

$$\mathcal{K}_{-+} = \mathcal{K}^*_{+-} = 0. \tag{B24}$$

We also state the expressions for the non-Galilean effective form factors for general polarization

$$\begin{aligned}\sum_{\lambda,\lambda'}\rho(\lambda,\lambda')\mathcal{E}_{\lambda'\lambda} = &\left(\frac{2}{3}+T_{LL}\right)\frac{t}{4}(\mathcal{G}_5(t)-\mathcal{G}_6(t)) + \left(\frac{1}{3}-T_{LL}\right)\frac{t}{2}(\mathcal{G}_5(t)+\mathcal{G}_6(t))\\ &+ iS_T\sin(\phi_S-\phi_t)\frac{M\sqrt{-t}}{2}\left[\left(1+\frac{t}{4M^2}\right)\mathcal{G}_5(t)+\frac{t}{4M^2}\mathcal{G}_6(t)\right]\\ &- T_{TT}\cos(2\phi_{T_T}-2\phi_t)\frac{t}{4}(\mathcal{G}_5(t)+\mathcal{G}_6(t)),\end{aligned} \tag{B25}$$

$$\sum_{\lambda,\lambda'}\rho(\lambda,\lambda')\mathcal{H}_{\lambda'\lambda} = \left[\left(\frac{2}{3}+T_{LL}\right)\frac{M^2t}{4}\left(1-\frac{t}{2M^2}\right) - \left(\frac{1}{3}-T_{LL}\right)\frac{M^2t}{2}\right. \tag{B26}$$

$$\left. - iS_T\sin(\phi_S-\phi_t)\frac{Mt\sqrt{-t}}{4} + T_{TT}\cos(2\phi_{T_T}-2\phi_t)\frac{M^2t}{4}\right]\mathcal{G}_6(t), \tag{B27}$$

$$\sum_{\lambda,\lambda'}\rho(\lambda,\lambda')\mathcal{K}_{\lambda'\lambda} = \left(S_L\frac{t}{8} + iT_{LT}\sin(\phi_{T_L}-\phi_t)\frac{M\sqrt{-t}}{2}\right)\mathcal{G}_6(t). \tag{B28}$$

APPENDIX C: SPIN-ONE DENSITY MATRIX

The density matrix $\rho(\lambda,\lambda')$ of a spin-one system is a 3×3 Hermitian matrix with unit trace, $\sum_{\lambda,\lambda'}\rho(\lambda,\lambda') = 1$. In the rest frame (RF) of the spin-one system it can be specified in a basis of single-particle states $|\boldsymbol{p}=\boldsymbol{0};\lambda\rangle$, where the momentum is zero and the spin is quantized along the z-axis, with spin projection $\lambda = (-1,0,1)$. The density matrix can be parametrized in the form [66]

$$\rho \equiv \rho(\lambda,\lambda') = \frac{1}{3} + \frac{1}{2}S_i\mathcal{S}_i + T_{ij}\mathcal{T}_{ij}. \tag{C1}$$

Here, $\mathcal{S}_i$ are the 3×3 matrices describing the spin operators in the spin-one representation for $\boldsymbol{e}_\pm = \mp\frac{1}{\sqrt{2}}(\boldsymbol{e}_x \pm i\boldsymbol{e}_y)$; $\boldsymbol{e}_0 = \boldsymbol{e}_z$,

$$\mathcal{S}_x = \frac{1}{\sqrt{2}}\begin{pmatrix}0&1&0\\1&0&1\\0&1&0\end{pmatrix},\qquad \mathcal{S}_y = \frac{i}{\sqrt{2}}\begin{pmatrix}0&-1&0\\1&0&-1\\0&1&0\end{pmatrix},\qquad \mathcal{S}_z = \begin{pmatrix}1&0&0\\0&0&0\\0&0&-1\end{pmatrix}, \tag{C2}$$

and their symmetric traceless rank-2 tensors

$$\mathcal{T}_{ij} = \frac{1}{2}(\mathcal{S}_i\mathcal{S}_j + \mathcal{S}_j\mathcal{S}_i) - \frac{2}{3}\delta_{ij}, \tag{C3}$$

and $i,j = (x,y,z)$ denote the Cartesian components. The parameters in Eq. (C1) are a three-dimensional vector S_i and a traceless symmetric tensor T_{ij}. They coincide, respectively, with the expectation value of the spin operators and their traceless tensor products

$$S_i = \mathrm{Tr}[\rho\hat{\mathcal{S}}_i] = \langle\hat{\mathcal{S}}_i\rangle, \tag{C4a}$$

$$T_{ij} = \mathrm{Tr}[\rho\hat{\mathcal{T}}_{ij}] = \langle\hat{\mathcal{T}}_{ij}\rangle. \tag{C4b}$$

In the rest frame of a particle, the covariant spin-one density matrix $\rho^{\beta\alpha}[RF]$ can be introduced as

$$\rho^{\beta\alpha}[RF] = \sum_{\lambda,\lambda'} \rho(\lambda,\lambda')\epsilon^{\beta}(k,\lambda)\epsilon^{*\alpha}(k,\lambda') = \frac{1}{3}\left(-g^{\beta\alpha} + \frac{k^{\beta}k^{\alpha}}{M^2}\right) - \frac{i}{2M}\epsilon^{\beta\alpha s[\mathrm{RF}]k} - t^{\beta\alpha}[\mathrm{RF}], \tag{C5}$$

where $k^{\mu} = (M, 0, 0, 0)$. In the rest frame, the spin vector $s^{\mu}[\mathrm{RF}]$ and tensor $t^{\beta\alpha}[\mathrm{RF}]$ only have spatial components, which are identical to the spin parameters appearing in Eq. (C1). The spin tensor is traceless. In formulas

$$s^{i}[\mathrm{RF}] \equiv S_i, \qquad s^{0}[\mathrm{RF}] = 0, \tag{C6a}$$

$$t^{ij}[\mathrm{RF}] \equiv T_{ij}, \qquad t^{0\alpha}[\mathrm{RF}] = t^{\beta 0}[\mathrm{RF}] = 0, \qquad t^{\mu}{}_{\mu}[\mathrm{RF}] = 0. \tag{C6b}$$

It is advantageous to consider the following $(2+1)$D (transverse, longitudinal) decomposition of the rest-frame spin vector and tensor,

$$S = (S_x, S_y, S_x) \equiv S_L(0,0,1) + S_T(\cos\phi_S, \sin\phi_S, 0), \tag{C7a}$$

$$T = \left(\begin{array}{cc|c} \frac{T_{xx}-T_{yy}}{2} - \frac{T_{zz}}{2} & T_{xy} & T_{xz} \\ T_{xy} & -\frac{T_{xx}-T_{yy}}{2} - \frac{T_{zz}}{2} & T_{yz} \\ \hline T_{xz} & T_{yz} & T_{zz} \end{array}\right) \equiv \left(\begin{array}{c|c} \boldsymbol{T}_{TT} - \frac{T_{LL}}{2}1_{2\times 2} & \boldsymbol{T}_{LT} \\ \hline \boldsymbol{T}_{LT} & T_{LL} \end{array}\right),$$

$$\boldsymbol{T}_{LT} = (T_{xz}, T_{yz}) \equiv T_{LT}(\cos\phi_{T_L}, \sin\phi_{T_L}), \tag{C7b}$$

$$\boldsymbol{T}_{TT} = \begin{pmatrix} \frac{T_{xx}-T_{yy}}{2} & T_{xy} \\ T_{xy} & -\frac{T_{xx}-T_{yy}}{2} \end{pmatrix} \equiv \frac{T_{TT}}{2}\begin{pmatrix} \cos 2\phi_{T_T} & \sin 2\phi_{T_T} \\ \sin 2\phi_{T_T} & -\cos 2\phi_{T_T} \end{pmatrix}, \tag{C7c}$$

where $\boldsymbol{T}_{TT}$ is symmetric and traceless in transverse coordinates.

In cases where one considers an outer product of two polarization vectors with specific helicity values λ, λ', one can obtain the value of $\epsilon^{\beta}(k,\lambda)\epsilon^{*\alpha}(k,\lambda')$ by making the following substitutions in Eq. (C5) for the unpolarized, vector and tensor polarized parts, see Eqs. (C4a) and (C4b),

$$1 \to \delta_{\lambda,\lambda'}, \tag{C8a}$$

$$S_i \to \langle\lambda'|\mathcal{S}_i|\lambda\rangle, \tag{C8b}$$

$$T_{ij} \to \langle\lambda'|\mathcal{T}_{ij}|\lambda\rangle. \tag{C8c}$$

Similar statements apply for the polarization parameters introduced in Eq. (C7).

For the case of particles with nonzero three-momentum we can introduce the density matrix by applying Lorentz boosts to the polarization four vectors in Eq. (C5) [17,46,66]. Different choices of standard boosts transforming the rest frame particle to the moving one result in different expressions for the polarization vectors (connected by the so-called Melosh rotations) [47,67]. As we consider the EMT on the light front, we only consider light front boosts $\Lambda_{\mathrm{LF}}(p)$ here

$$\begin{aligned}\rho^{\beta\alpha}(p) &= \sum_{\lambda,\lambda'} \rho(\lambda,\lambda')\Lambda_{\mathrm{LF}}(p)^{\beta}{}_{\mu}\epsilon^{\mu}(k,\lambda)\Lambda_{\mathrm{LF}}(p)^{\alpha}{}_{\nu}\epsilon^{*\nu}(k,\lambda') \\ &= \sum_{\lambda,\lambda'} \rho(\lambda,\lambda')\epsilon^{\beta}(p,\lambda)\epsilon^{*\alpha}(p,\lambda') = \frac{1}{3}\left(-g^{\beta\alpha} + \frac{p^{\beta}p^{\alpha}}{M^2}\right) - \frac{i}{2M}\epsilon^{\beta\alpha s p} - t^{\beta\alpha},\end{aligned} \tag{C9}$$

where the covariant spin vector and tensor are introduced as

$$p^{\mu} = \Lambda_{\mathrm{LF}}(p)^{\mu}{}_{\nu}k^{\mu}, \qquad s^{\mu} = \Lambda_{\mathrm{LF}}(p)^{\mu}{}_{\nu}s^{\nu}[\mathrm{RF}], \qquad (sp) = 0, \tag{C10a}$$

$$t^{\mu\nu} = \Lambda_{\rm LF}(p)^{\mu}{}_{\rho}\Lambda_{\rm LF}(p)^{\nu}{}_{\sigma}t^{\rho\sigma}[\mathrm{RF}], \qquad t^{\beta\alpha}p_{\alpha} = p_{\beta}t^{\beta\alpha} = 0, \qquad t^{\mu}{}_{\mu} = 0. \tag{C10b}$$

To compute the spatial densities of the EMT, we need off-diagonal bilinears of spin-one polarization four vectors. We therefore need the expression for the off-diagonal covariant density matrix. We write this expression using the averaged spin vector $\bar{s}$ and tensor $\bar{t}$ [68], which are obtained by boosting the rest frame ones of Eq. (C6) with the average momentum $P = \frac{p+p'}{2}$,

$$\bar{s}^{\mu} = \Lambda_{\rm LF}(P)^{\mu}{}_{\nu}s^{\nu}[\mathrm{RF}], \tag{C11a}$$

$$\bar{t}^{\mu\nu} = \Lambda_{\rm LF}(P)^{\mu}{}_{\rho}\Lambda_{\rm LF}(P)^{\nu}{}_{\sigma}t^{\rho\sigma}[\mathrm{RF}]. \tag{C11b}$$

The off-diagonal density matrix then becomes

$$\begin{aligned}
\rho^{\beta\alpha}_{\rm LF}(p,p') &= \sum_{\lambda,\lambda'}\rho(\lambda,\lambda')\Lambda_{\rm LF}(p)^{\beta}{}_{\mu}\epsilon^{\mu}(k,\lambda)\Lambda_{\rm LF}(p')^{\alpha}{}_{\nu}\epsilon^{*\nu}(k,\lambda') \\
&= \frac{1}{3}\left[-g^{\beta\alpha} + \frac{P^{\beta}P^{\alpha}}{M^2} - \frac{\Delta^{\beta}\Delta^{\alpha}}{4M^2} + \frac{P^{[\beta}\Delta^{\alpha]}}{2M^2} + \frac{\Delta^{[\beta}n^{\alpha]} + \xi\Delta^{\{\beta}n^{\alpha\}}}{(1-\xi^2)(P\cdot n)} + \frac{\Delta^2}{2(1-\xi^2)}\frac{n^{\beta}n^{\alpha}}{(P\cdot n)^2}\right] \\
&\quad + \frac{i}{2MD}\left\{\epsilon^{\beta\alpha\bar{s}P} - (D-1)(\bar{s}\cdot n)\frac{M^2}{(P\cdot n)^2}\epsilon^{\beta\alpha+P} - (D-1)\frac{P^{[\beta}\epsilon^{\alpha]n\bar{s}P}}{(P\cdot n)} + \frac{D}{2}\frac{\Delta^{\{\beta}\epsilon^{\alpha\}n\bar{s}P}}{(P\cdot n)}\right. \\
&\quad - D(D-1)\frac{M^2}{(1-\xi^2)(P\cdot n)^2}(n^{[\beta}\epsilon^{\alpha]n\bar{s}P} - \xi n^{\{\beta}\epsilon^{\alpha\}n\bar{s}P}) + \frac{\epsilon^{n\Delta\bar{s}P}}{2(1-\xi^2)(P\cdot n)^2}\left[-2D(D-1)\frac{M^2}{(P\cdot n)}n^{\beta}n^{\alpha}\right. \\
&\quad \left. - (D-1)(P^{\{\beta}n^{\alpha\}} + \xi P^{[\beta}n^{\alpha]}) + \frac{D}{2}(\Delta^{[\beta}n^{\alpha]} + \xi\Delta^{\{\beta}n^{\alpha\}})\right] - \frac{n^{\{\beta}\epsilon^{\alpha\}\Delta\bar{s}P} - \xi n^{[\beta}\epsilon^{\alpha]\Delta\bar{s}P}}{2(1-\xi^2)(P\cdot n)} \\
&\quad \left. + (D-1)\frac{(\bar{s}\cdot n)}{(P\cdot n)}M^2\frac{n^{\{\beta}\epsilon^{\alpha\}\Delta nP} - \xi n^{[\beta}\epsilon^{\alpha]\Delta nP}}{2(1-\xi^2)(P\cdot n)^2}\right\} - \bar{t}^{\beta\alpha} + \frac{\Delta^{[\beta}\bar{t}^{\alpha]n}}{2(P\cdot n)} - \frac{n^{[\beta}\bar{t}^{\alpha]\Delta} - \xi n^{\{\beta}\bar{t}^{\alpha\}\Delta}}{2(1-\xi^2)(P\cdot n)} + \bar{t}^{nn}\frac{\Delta^{\beta}\Delta^{\alpha}}{4(P\cdot n)^2} \\
&\quad - \bar{t}^{n\Delta}\frac{n^{\{\beta}\Delta^{\alpha\}} - \xi n^{[\beta}\Delta^{\alpha]}}{4(1-\xi^2)(P\cdot n)^2} + \bar{t}^{\Delta\Delta}\frac{n^{\beta}n^{\alpha}}{4(1-\xi^2)(P\cdot n)^2},
\end{aligned} \tag{C12}$$

where

$$D = \sqrt{1 - \frac{t}{4M^2}}, \tag{C13a}$$

$$a^{\{\mu}b^{\nu\}} = a^{\mu}b^{\nu} + a^{\nu}b^{\mu}, \qquad a^{[\mu}b^{\nu]} = a^{\mu}b^{\nu} - a^{\nu}b^{\mu}. \tag{C13b}$$

[1] X.-D. Ji, Phys. Rev. Lett. **74**, 1071 (1995).
[2] X.-D. Ji, Phys. Rev. D **52**, 271 (1995).
[3] C. Lorcé, Eur. Phys. J. C **78**, 120 (2018).
[4] Y. Hatta, A. Rajan, and K. Tanaka, J. High Energy Phys. 12 (2018) 008.
[5] A. Metz, B. Pasquini, and S. Rodini, Phys. Rev. D **102**, 114042 (2020).
[6] X. Ji, Front. Phys. **16**, 64601 (2021).
[7] C. Lorcé, A. Metz, B. Pasquini, and S. Rodini, J. High Energy Phys. 11 (2021) 121.
[8] J. Ashman *et al.* (European Muon Collaboration), Phys. Lett. B **206**, 364 (1988).
[9] X.-D. Ji, Phys. Rev. Lett. **78**, 610 (1997).
[10] E. Leader and C. Lorcé, Phys. Rep. **541**, 163 (2014).
[11] M. V. Polyakov, Phys. Lett. B **555**, 57 (2003).
[12] I. A. Perevalova, M. V. Polyakov, and P. Schweitzer, Phys. Rev. D **94**, 054024 (2016).
[13] M. V. Polyakov and P. Schweitzer, Int. J. Mod. Phys. A **33**, 1830025 (2018).

[14] W. Boeglin and M. Sargsian, Int. J. Mod. Phys. E **24**, 1530003 (2015).
[15] R. L. Jaffe and A. Manohar, Phys. Lett. B **223**, 218 (1989).
[16] S. K. Taneja, K. Kathuria, S. Liuti, and G. R. Goldstein, Phys. Rev. D **86**, 036008 (2012).
[17] W. Cosyn, S. Cotogno, A. Freese, and C. Lorcé, Eur. Phys. J. C **79**, 476 (2019).
[18] M. V. Polyakov and B.-D. Sun, Phys. Rev. D **100**, 036003 (2019).
[19] J.-Y. Kim, B.-D. Sun, D. Fu, and H.-C. Kim, arXiv:2208.01240.
[20] Z. Abidin and C. E. Carlson, Phys. Rev. D **77**, 095007 (2008).
[21] A. Freese and I. C. Cloët, Phys. Rev. C **100**, 015201 (2019).
[22] B.-D. Sun and Y.-B. Dong, Phys. Rev. D **101**, 096008 (2020).
[23] E. Epelbaum, J. Gegelia, U. G. Meißner, and M. V. Polyakov, Phys. Rev. D **105**, 016018 (2022).
[24] G. N. Fleming, Charge distributions from relativistic form-factors, in *Physical Reality and Mathematical Description: Festschrift Jauch (Josef Maria) on his 60th Birthday*, edited by C. P. Enz and J. Mehra (D. Reidel Publishing Company, Dordrecht, Holland, 1974), pp. 357–374.
[25] M. Burkardt, Int. J. Mod. Phys. A **18**, 173 (2003).
[26] G. A. Miller, Phys. Rev. C **99**, 035202 (2019).
[27] C. Lorcé, H. Moutarde, and A. P. Trawiński, Eur. Phys. J. C **79**, 89 (2019).
[28] R. L. Jaffe, Phys. Rev. D **103**, 016017 (2021).
[29] C. Lorcé, Phys. Rev. Lett. **125**, 232002 (2020).
[30] A. Freese and G. A. Miller, Phys. Rev. D **103**, 094023 (2021).
[31] E. Epelbaum, J. Gegelia, N. Lange, U. G. Meißner, and M. V. Polyakov, Phys. Rev. Lett. **129**, 012001 (2022).
[32] G. A. Miller, Phys. Rev. Lett. **99**, 112001 (2007).
[33] G. A. Miller, Phys. Rev. C **80**, 045210 (2009).
[34] A. Freese and W. Cosyn, following paper, Phys. Rev. D **106**, 114014 (2022).
[35] B. R. Holstein, arXiv:gr-qc/0607054.
[36] A. Freese, arXiv:2112.00047.
[37] E. R. Berger, F. Cano, M. Diehl, and B. Pire, Phys. Rev. Lett. **87**, 142302 (2001).
[38] C. E. Carlson and M. Vanderhaeghen, Eur. Phys. J. A **41**, 1 (2009).
[39] A. D. Poularikas, *Transforms and Applications Handbook* (CRC Press, Boca Raton, FL, 2018).
[40] C. Lorcé, Eur. Phys. J. C **78**, 785 (2018).
[41] J. M. B. Kellogg, I. I. Rabi, N. F. Ramsey, and J. R. Zacharias, Phys. Rev. **55**, 318 (1939).
[42] C. Lorcé and P. Wang, Phys. Rev. D **105**, 096032 (2022).
[43] F. Cano and B. Pire, Eur. Phys. J. A **19**, 423 (2004).
[44] W. Cosyn, Y.-B. Dong, S. Kumano, and M. Sargsian, Phys. Rev. D **95**, 074036 (2017).
[45] W. Cosyn and B. Pire, Phys. Rev. D **98**, 074020 (2018).
[46] W. Cosyn and C. Weiss, Phys. Rev. C **102**, 065204 (2020).
[47] H. J. Melosh, Phys. Rev. D **9**, 1095 (1974).
[48] H. Leutwyler and J. Stern, Ann. Phys. (N.Y.) **112**, 94 (1978).
[49] P. Masjuan, E. Ruiz Arriola, and W. Broniowski, Phys. Rev. D **87**, 014005 (2013).
[50] D. A. Pefkou, D. C. Hackett, and P. E. Shanahan, Phys. Rev. D **105**, 054509 (2022).
[51] A. Freese and G. A. Miller, Phys. Rev. D **104**, 014024 (2021).
[52] Y. Chen and C. Lorcé, arXiv:2210.02908.
[53] I. Sick and D. Trautmann, Nucl. Phys. **A637**, 559 (1998).
[54] R. F. Code and N. F. Ramsey, Phys. Rev. A **4**, 1945 (1971).
[55] D. M. Bishop and L. M. Cheung, Phys. Rev. A **20**, 381 (1979).
[56] T. E. O. Ericson and M. Rosa-Clot, Nucl. Phys. **A405**, 497 (1983).
[57] V. D. Burkert, L. Elouadrhiri, and F. X. Girod, Nature (London) **557**, 396 (2018).
[58] R. Binder, *Fluid Mechanics*, Prentice-Hall engineering series (Prentice-Hall, Englewood Cliffs, NJ, 1943).
[59] A. Airapetian *et al.* (HERMES Collaboration), Nucl. Phys. **B829**, 1 (2010).
[60] A. Airapetian *et al.* (HERMES Collaboration), Nucl. Phys. **B842**, 265 (2011).
[61] M. Mazouz *et al.* (Jefferson Lab Hall A Collaboration), Phys. Rev. Lett. **118**, 222002 (2017).
[62] W. Armstrong *et al.*, arXiv:1708.00888.
[63] C. Muñoz Camacho *et al.*, JLab12 proposal: PR12-22-006 (2022).
[64] D. Boer *et al.*, arXiv:1108.1713.
[65] R. Abdul Khalek *et al.*, Nucl. Phys. **A1026**, 122447 (2022).
[66] E. Leader, *Spin in Particle Physics*, Cambridge Monographs on Particle Physics, Nuclear Physics and Cosmology (Cambridge University Press, Cambridge, England, 2005).
[67] W. N. Polyzou, W. Glöckle, and H. Witala, Few Body Syst. **54**, 1667 (2013).
[68] C. Lorcé, Phys. Rev. D **97**, 016005 (2018).